Ruthenium(III) vs Palladium(II) N_2O_2 Schiff Base Complexes: Catalytic Efficiency - A Comparative Analysis

V. Raji[a,b] , Neetu Pradeep[a,b] , Vasudevan Arun[a, b]

[a]Department of Chemistry, Sree Narayana College, Punalur-691305 (Affiliated to University of Kerala), Kollam, Kerala, India.

[b]Research Department of Chemistry, Sree Narayana College, Kollam-691001, (Affiliated to University of Kerala), Kerala, India

Abstract:

N_2O_2 Schiff base complexes of Ruthenium(III) and Palladium(II) are widely studied for their catalytic potential in oxidation reactions. These complexes, equipped with nitrogen and oxygen donor atoms, stabilize metal centers and enable catalytic applications across organic synthesis, fine chemical production, and green chemistry. This review comprehensively examines the catalytic efficiency of Ruthenium(III) and Palladium(II) complexes, identifying their unique redox properties and structural attributes as key factors influencing activity. For instance, Ruthenium(III) complexes excel in redox-based reactions due to their ability to shift between oxidation states, enhancing reaction rates and selectivity in oxidation reactions. In contrast, Palladium(II) complexes are known for their stability in coupling reactions, which rely on their stable coordination geometry to facilitate carbon-carbon bond formation. A comparative analysis reveals Ruthenium(III) complexes generally outperform in oxidation catalysis, owing to their adaptable redox states and efficient electron transfer capabilities. This review seeks to clarify the structural and mechanistic properties that govern catalytic efficiency by evaluating these complexes, offering insights into optimizing catalytic systems for advanced applications.

Keywords: Redox properties, Organic synthesis, Electron transfer, Alcohol oxidation, Mechanistic properties

Graphical Abstract

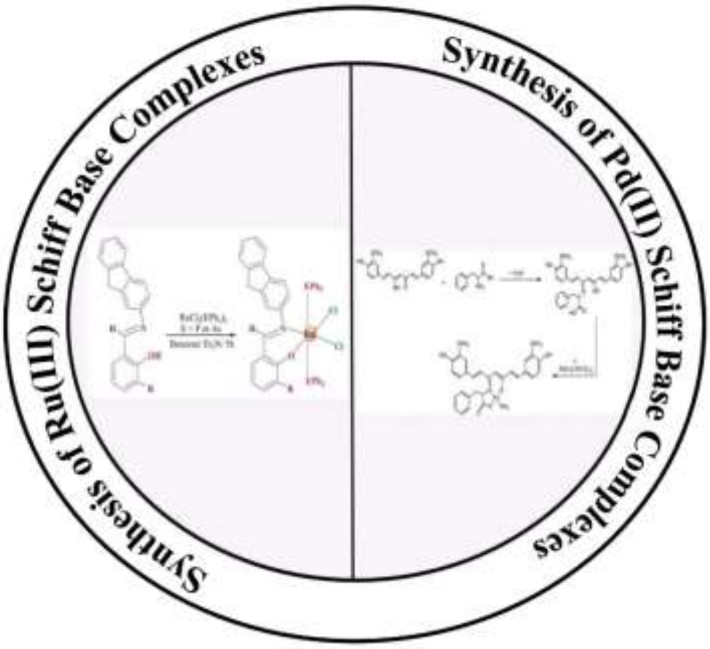

1. INTRODUCTION

1.1 Background on N_2O_2 Schiff base complexes

Schiff base complexes with an N_2O_2 donor set have become integral in catalysis due to their tunable properties and versatility in coordinating with metal centers. Schiff bases, which result from condensation of amines with carbonyl compounds (typically aldehydes or ketones), can form stable chelates when bound to metals (1), (2). The N_2O_2 framework in particular consisting of two nitrogen and two oxygen donor atoms offers a balanced electron-donating environment that stabilizes the central metal ion, whether in a low or high oxidation state. These complexes are known for their structural flexibility and ability to adopt various geometries, such as square planar or octahedral, depending on the metal and its coordination environment (3). This adaptability allows Schiff base ligands to effectively support transition metals in catalytic cycles, making them popular in oxidation and reduction reactions, hydrolysis, and other processes essential to organic synthesis and industrial applications (4) (5). Ruthenium (III) and palladium (II) are two metals frequently used with N_2O_2 Schiff base ligands due to its distinct redox and catalytic properties. Ruthenium, with its accessible oxidation states, excels in redox reactions, making it a prime choice for catalytic oxidation of organic molecules. Palladium, however, is renowned for its role in carbon-carbon coupling reactions, such as Suzuki and Heck reactions, due to its unique oxidative addition and reductive elimination capabilities. The structural integrity and ligand field provided by the N_2O_2 Schiff base ligands not only enhance the stability of ruthenium and palladium complexes but also significantly impact the reaction rates and selectivity of catalytic transformations. This balance of stability and reactivity makes N_2O_2 Schiff base complexes highly efficient in diverse applications across chemistry and material science (6), (7), (8), (9).

1.2. Importance of catalysis in oxidation reactions

Catalysis in oxidation reactions is critical in both industrial and environmental applications due to its efficiency in transforming organic molecules into more functionalized or oxidized forms. Oxidation reactions are foundational in chemical manufacturing, especially in producing fine chemicals, pharmaceuticals, and polymers. Catalysts streamline these reactions by lowering the activation energy, which enhances reaction rates and improves yields while minimizing waste. This efficiency is vital for sustainable practices, as it reduces energy consumption and the need for harsh reagents, thus lowering the environmental footprint of these processes.

Transition metal catalysts, such as those incorporating ruthenium and palladium, are particularly valuable in oxidation. Their variable oxidation states allow them to facilitate electron transfer between reactants, which is key in oxidation processes. For example, ruthenium-based catalysts are widely used in selective oxidations of alcohols to aldehydes or ketones, essential step in many synthetic pathways. Similarly, palladium catalysts support the oxidation of hydrocarbons and other substrates under milder conditions than traditional methods, contributing to greener chemical synthesis. The development and refinement of oxidation catalysts continue to expand their applications in creating more efficient, cost-effective, and environmentally friendly chemical processes.

1.3. Objective:

- To compare the analysis of Ru(III) an Pd(II) complexes

The purpose of this analysis is to compare the catalytic efficiency of palladium (II) and ruthenium (III) complexes, with an emphasis on how well they function in oxidation processes. We evaluate the degree to which each metal complex facilitates catalytic conversions by looking at important variables including coordination geometry, redox characteristics, turnover frequencies (TOFs), and turnover numbers (TONs). Pd(II) complexes are excellent in carbon-carbon coupling processes, but Ru(III) complexes are frequently effective at oxidizing alcohols and sulfides. This comparative analysis sheds light on the best catalysts to use in particular organic processes.

2. CATALYTIC EFFICIENCY: RUTHENIUM(III) COMPLEXES

2.1 Redox properties and coordination geometry

Ruthenium(III) complexes are highly effective in catalysis due to their versatile redox properties and flexible coordination geometry. The ability of ruthenium to exist in multiple oxidation states, commonly ranging from +2 to +4, allows it to participate readily in redox reactions. This multivalency is crucial in catalytic cycles, particularly in oxidation and reduction reactions, as it enables ruthenium to shuttle between oxidation states to facilitate electron transfer. In oxidative catalysis, for example, ruthenium(III) complexes can be easily oxidized to ruthenium(IV) intermediates, allowing them to interact with substrates and form products before reverting to their initial state. Regarding coordination geometry, ruthenium(III) complexes by N_2O_2 Schiff base ligands typically adopt square planar or octahedral configuration, depending on the ligand environment and other coordinating atoms. The square planar geometry is especially favorable in Schiff base complexes as it enhances orbital overlap between the metal and ligand, stabilizing the complex and promoting catalytic reactivity. Additionally, the flexibility of ruthenium to adjust its coordination geometry in response to different substrates aids in catalytic efficiency, allowing it to adapt to a range of molecular structures and support diverse reaction pathways. This adaptability and its robust redox properties make ruthenium(III) Schiff base complexes powerful catalysts on oxidation reactions.

All binuclear ruthenium(III) Schiff base complexes exhibit two consecutive quasi-reversible oxidation pairs instead of reduction waves at negative potentials $(Ru_2^{IV,IV}\text{-}Ru_2^{III,III})$. The redox potentials facilitate quasi-reversibility and are independent of different scan rates. For each complex, distinct half wave-potentials were found that corresponded to the first and second oxidation couples. It was discovered that the first oxidation was caused by ruthenium (III) centers oxidizing to proper mixed-valence complex (10).

$$[(EPh_3)(X)\text{-}Ru^{III}\text{-}Y\text{-}Ru^{III}\text{-}(X)(EPh_3)] \rightleftharpoons [(EPh_3)(X)\text{-}Ru^{III}\text{-}Y\text{-}Ru^{III}\text{-}(X)(EPh_3)] \qquad (1)$$

The substitution of $AsPh_3$ for PPh_3 and the characteristics of the bridging ligand in the complexes have been shown to cause no difference in redox potentials.

Using cyclic voltammetry, complexes' redox behavior investigated in dichloromethane at working electrode of glassy carbon (Table 1). The Schiff base complexes' redox capacities are distinguished through distinct waves that fall between 0.81 and 1.03 V for oxidation also between -0.32 and -0.73 V for reduction, respectively, with SCE (Figure 1). The metal-centered Ru^{III}–Ru^{II} and Ru^{IV}–Ru^{III} couples are attributed with redox waves as ligands remain quiescent during potential choice of +2.0 V to -2.0 V. This oxidation almost reversible, through peak-to-peak separation (ΔEp) of 150 – 400 mV. This caused by delayed electron transit also complicated adsorption onto surface of electrode. Typically, these compounds exhibit an irreversible reduction peak and a single quasi-reversible oxidation pair. Irreversible cyclic voltammograms are displayed by the complexes' reduction processes (Ru^{III}–Ru^{II}). These findings suggest that the Ru^{III}–Ru^{II} pair's charge transfer mechanism is often slower than that of the Ru^{IV}–Ru^{III} couple. The irreversibility of complexes could due to reductive breakdown or the metal ion's transient reduced state. The complexes' replacement of triphenylarsine for triphenylphosphine has likewise been shown to result in minimal alteration in the redox potentials. Recent observations of additional ruthenium (III) complexes have shown similar behavior (11),(12).

Table 1: Cyclic Voltammetric Data for Schiff base complexes of ruthenium (III) (Saridha et al., 2005)

Complex	Ru^{III}-Ru^{IV}				Ru^{III}-Ru^{II}			
	$E_{pa}(V)$	$E_{pc}(V)$	$\Delta E_p(mV)$	$E_{1/2}(V)$	$E_{pa}(V)$	$E_{pc}(V)$	$\Delta E_p(mV)$	$E_{1/2}(V)$
(1)	1.0	0.79	210	0.895	-	-0.36	-	-
(3)	1.13	0.73	400	0.930	-	-0.73	-	-
(5)	1.03	0.87	160	0.950	-	-0.50	-	-
(8)	1.08	0.85	230	0.965	-	-0.65	-	-

Supporting electrolyte: $[NBu_4]ClO_4$ (0.1 M). Scan rate: 100mV s^{-1}.
Reference electrode: Ag/AgCl.

$$\Delta E_p = E_{pa} - E_{pc} \qquad (2)$$

$$E_{1/2} = 0.5\,(E_{pa} + E_{pc}) \qquad (3)$$

where E_{pc} and E_{pa} are cathodic as well as anodic peak potentials in V, respectively.

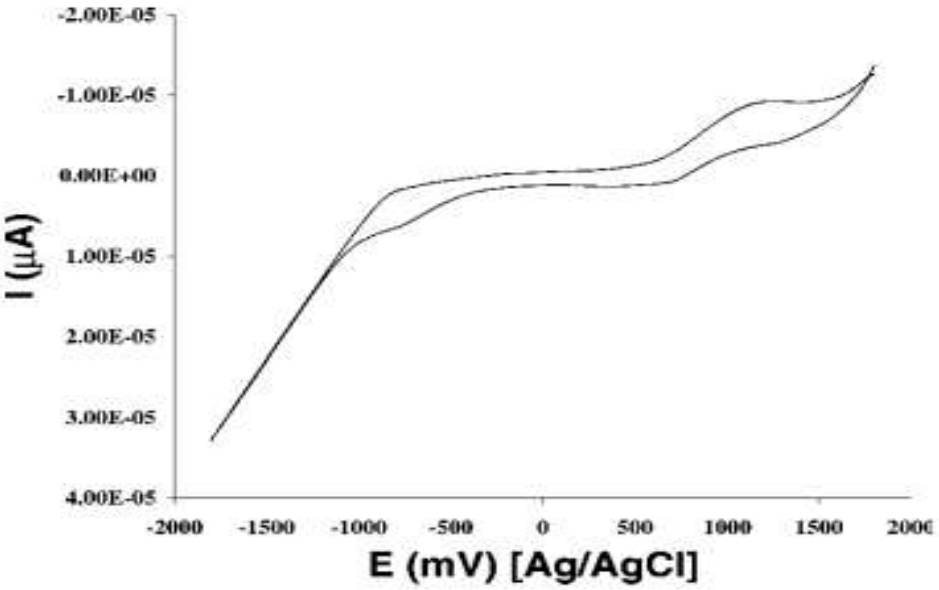

Figure. 1. Cyclic voltammogram of Schiff base complex of Ru^{III} (Saridha et al., 2005)

2.2 High turnover frequencies (TOFs) and turnover numbers (TONs)

Ruthenium(III) complexes are notable for their high TOF and TON in catalysis, which make them highly efficient catalysts for various reactions, especially oxidations. TOF, the quantity of substrate molecules that are transformed for every catalyst molecule in a certain amount of time, is an indicator of reaction speed and efficiency. High TOFs in ruthenium(III) complexes stem from their ability to undergo rapid redox cycling between oxidation states, enabling them to engage substrates quickly and return to the active catalytic state. This rapid cycling, combined with their inherent stability, contributes to faster reaction rates, which is beneficial for both small-scale and industrial applications where time efficiency is essential.

The turnover number (TON), which represents the total number of substrate molecules converted by a single catalyst molecule before deactivation, is also high for ruthenium(III) Schiff base complexes. The robust N_2O_2 coordination environment helps stabilize ruthenium in various redox states, extending the catalyst's operational lifespan and allowing it to participate in multiple catalytic cycles without significant degradation. This high TON value reduces the amount of catalyst required, making ruthenium(III) complexes more cost-effective and sustainable for applications that require prolonged reaction times. The combination of high TOFs and TONs in ruthenium(III) complexes thus underscores their efficiency and effectiveness as catalysts in organic transformations, particularly in oxidation reactions.

2.3 Efficient oxidation of alcohols

Efficient oxidation of alcohols is a critical transformation in organic chemistry, converting alcohols to valuable aldehydes, ketones, or carboxylic acids used in pharmaceuticals, fragrances, and agrochemicals. Catalysts, particularly metal complexes, enhance this process by lowering reaction energy barriers, allowing for selective, rapid oxidation under milder conditions, reducing waste, and making the process more sustainable and economically viable. Eq. 4 displays the oxidation of alcohols catalyzed by NMO and Binuclear Ruthenium (III) Schiff base complexes (13).

$$1^{\circ}(\mathrm{or})2^{\circ}\,alcohols \xrightarrow[reflux/8\text{-}12h:\,CH_2\,Cl_2]{\substack{L=[Ru_2Cl_2(PPh_3)_2(L)](0.4mol\%)\\ Bis\text{-}salophen(1),\,Bis\text{-}naphophen(5)}} Aldehydes(\mathrm{or})Ketone \qquad (4)$$

Table 2: Alcohols are catalytically oxidized by the binuclear ruthenium(III) Schiff base complex $[Ru_2Cl_2(PPh_3)2(L1)]$ (1) and $[Ru_2Cl_2(PPh_3)2(L2)]$ (5) with NMO present. (14).

Entry	Substrate (A)	Product (K)	Yield (%)	TON[f]
1	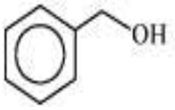 Benzyl alcohol	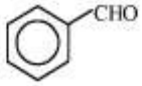 Benzaldehyde	A= 41 B= 39	A= 102 B= 98
2	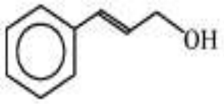 phenylpropanol	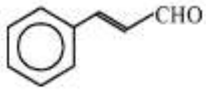 cinnamaldehyde	A= 38.4 B= 64.8	A= 96 B= 162
3	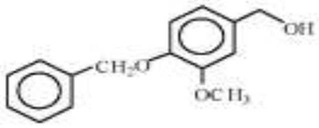 4-hydroxy-3-methoxyphenyl(phenyl)methane	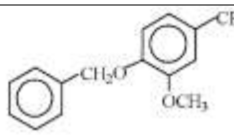 4-hydroxy-3-methoxybenzaldehyde	A= 90 B=64	A= 225 B= 160
4	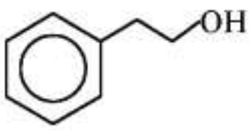 3-phenyl-1-propanol	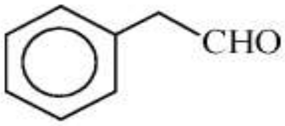 benzaldehyde	A = 18.5 B = 46	A= 46 B= 115
5	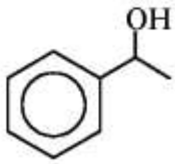 1-phenylethanol	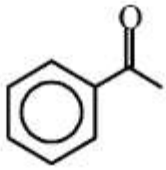 acetophenone	A= 85[c] B = 84[c]	A= 212 B= 210

[c] Moles of product per mole of catalyst. [f] TON, moles of product/moles of catalyst.

The ability of Schiff base complexes of binuclear ruthenium (III) $[Ru_2Cl_2(PPh_3)_2(L1)]$ (1) as well as $[Ru_2Cl_2(PPh_3)_2(L2)]$ (5) to catalyze oxidation of many main and subordinate alcohols (Table 2) when oxidant NMO (Eq.4) was present. Following the completion of the oxidation process in CH_2Cl_2, water was removed with powdered molecular sieves. The outcomes of current investigation advise that complexes' effective reaction through NMO as intermediate in ruthenium complexes catalyzed oxidation by NMO result in production of high valent ruthenium-oxo-species.

The reaction mixture's colour different from reddish brown to green upon addition of NMO to solution of binuclear ruthenium(III) Schiff base complexes in CH_2Cl_2 signifying emergence of new species. Following proper reflux duration, the aldehyde or ketones were identified b Gas Chromatography (GC) analysis using real materials or measured as 2,4-dinitrophenylhydrazone derivatives. Control tests demonstrated the alcohols did not oxidize when the co-oxidant NMO or the binuclear ruthenium(III) Schiff base complexes were absent. The catalytic oxidation process that turns benzyl alcohol into benzaldehyde by traces of benzoic acid showed minimal activity for both complexes 1 and 5. Cinnamyl alcohol was also shown to convert to cinnamon aldehyde with traces of cinnamic acid. However, for complexes 1 and 5, this catalytic system effectively oxidizes 3-methoxy-4-benzyloxybenzyl alcohol in 8 hours (90% and 64%, respectively).

In case of 1-phenyl ethanol, GC analysis using genuine samples allowed for the identification of the resultant product, acetophenone, also both complexes exhibit good activity by conversion rates of 85% and 84%, respectively. The isolated yield of these complexes is up to 92.7%. Likewise, benzoin and diphenyl carbinol, which are secondary alcohols, converted to their respective ketones by a reasonable to high yield. Cyclic alcohols, such as cycloheptanol, cyclohexanol, cyclooctanol, and cyclopentanol, made up to 84%, were successfully oxidized to matching ketones by binuclear ruthenium (III) Schiff base complexes 1 and 5. In case of allylic alcohols, very little product was generated even after 12 hours. The fact that cinnamonyl alcohol produced a 64.8% yield in similar catalytic structure in 8 hours suggests that there may not have been conjugation. Additionally, cholesterol is catalyzed to cholestenone by complexes 1 and 5, with conversion rates of 54% and 43.7%, respectively. These findings demonstrated that, as seen in figure 2, In the current catalytic system, secondary alcohols oxidize more effectively to their corresponding ketones than primary alcohols on their equivalent aldehydes (15).

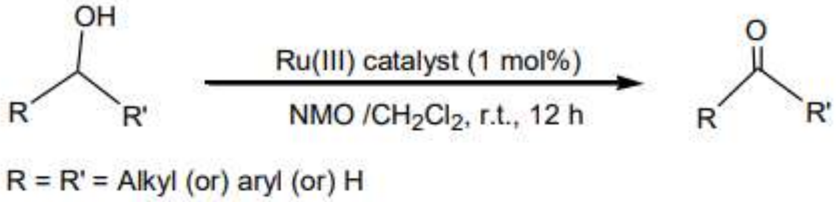

Figure 2: Alcohols' catalytic oxidation reactions to aldehydes and ketones (16).

2.4 Efficient Oxidation of Alkenes

When an oxidant is applied to a low-valent ruthenium catalyst, middle-valent Ru=O species are produced. These species frequently exhibit reactivity that differs from that of the RuO_4 oxidation. Metalloporphyrin-induced alkene epoxidation has been investigated as a cytochrome P-450 model process (17). The catalytic oxidation of styrene with $PhIO$ has been investigated for ruthenium porphyrins, such as $Ru(OEP)(PPh_3)Br$ (OEP = octaethylporphyrinato) (Matteucci et al., 2003). The corresponding epoxides were produced in great quantities when alkenes were oxidized by 2,6-dichloropyridine N-oxide under influence of ruthenium porphyrin [Eqs. (5) and 6)]. The ruthenium coordinates more strongly with plain pyridine, slowing down catalysis, hence substituents at positions two and six on pyridine N-oxide are essential for greator efficiency. When a ruthenium porphyrin catalyst is present, nitrous oxide (N_2O) could also be utilized as an oxidant to epoxidize trisubstituted olefins (18).

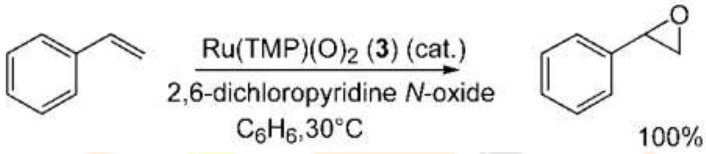

(5)

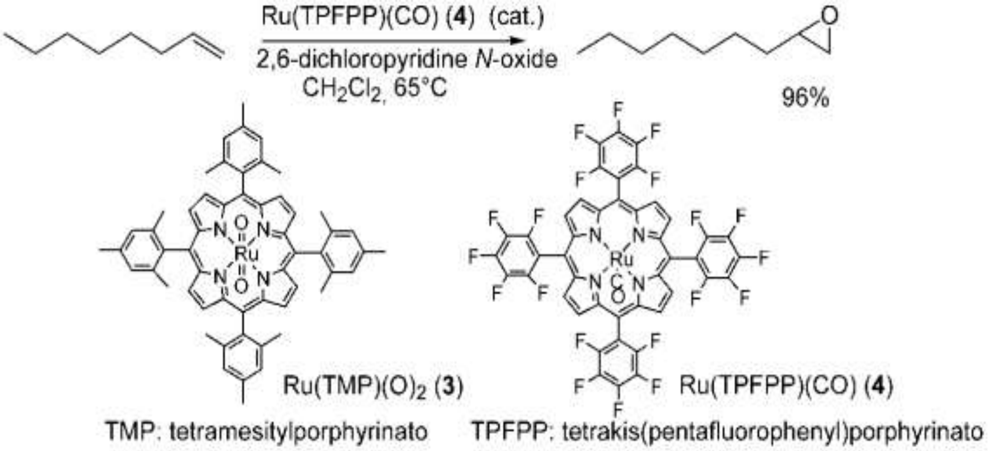

(6)

Alkene oxidations with PhIO are catalyzed by non-porphyrin ruthenium complexes like $[RuCl(DPPP)_2]$($DPPP$=1,3-bis(di-phenylphosphino) propane) as well as $[Ru(6{,}6\text{-}Cl_2)_2(H_2O)_2]$.

Many groups have looked into the aerobic oxidation of alkenes with ruthenium. At 1 atm of molecular oxygen, $Ru(TMP)(O)_2$ (3) catalyzes the aerobic epoxidation of alkenes without the need of a reducing agent. Additionally useful for epoxidation with molecular oxygen are Ru-containing polyoxometalate, $\{[WZnRu_2(OH)(H_2O)](ZnW_9O_{34})_2\}^{11-}$ (19), also sterically hindered ruthenium complex, $[Ru(dmp)_2(CH_3CN)_2](PF_6)$ (dmp = 2,9-dimethyl-1,10-phenanthroline) (Lindén et al., 2003). In a perfluorinated solvent containing $i\text{-}PrCHO$, alkenes undergo aerobic epoxidation catalyzed by a ruthenium catalyst with perfluorinated 1,3-diketone ligands. By ruthenium complexes with oxidants such as $PhIO$, $PhI(OAc)_2$, 2,6-dichloropyridine N-oxide, as well as molecular oxygen, asymmetric epoxidations have been reported (20).

A novel kind of catalytic oxidation of alkenes could carried out if intermediate 5 could be trapped with an exogenous nucleophile, like water. It was found that the conversion of alkenes into -ketols proceeds quite effectively. Therefore, the corresponding -ketols, that are important structural components of several compounds that are physiologically active, are produced when alkenes and peracetic acid undergo moderate oxidation in an aqueous solution catalyzed by low-valent ruthenium [Eq. (7)] (21).

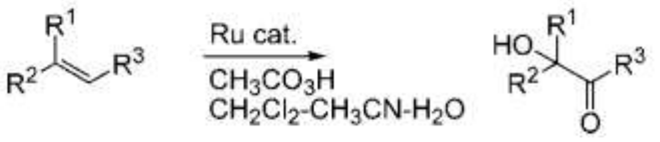

(7)

2.5 Efficient oxidation of sulfides

White LED irradiation (λ >380 nm) was used to execute Sulfide oxidation driven by light using a complex (2 or 3) and Co(III)24 as a sacrificial electron acceptor in deoxygenated phosphate buffer (0.1 M, pH 6.8): substrate A mole ratio of 1:1000:2000 for Co(III) at room temperature. Using H NMR spectroscopy and dichloromethane, the appropriate compounds were extracted. Sulfide was converted with 99% product selectivity to the equivalent sulfoxide in the form of a 4-methoxythioanisole substrate. Following 8 hours of irradiation, a TON of up to 709 based on Ru_{phot}−Ru_{cat}−H_2O was achieved. The precatalyst, Ru_{phot}−Ru_{cat}−Cl, would quickly swap Cl^{-}/H_2O ligands to transform into its aqua form under the same conditions, resulting in a decreased efficiency with a TON of 645, as shown in Figures 3 and 4. Compared to the supramolecular system under the same reaction conditions,

The catalytic photooxidation of sulfide in solution including $[Ru(bpy)_3]^{2+}$(0.01 mM), $[Ru(tpy)\text{-}(bpy)H_2O]^{2+}$ (0.01 mM), Co(III) (20 mM), and 4-methoxythioanisole (10 mM) had substantially lower TONs (only 101 after 8 hours). In solution includes $[Ru(bpy)_3]^{2+}$(0.01 mM), $[Ru(tpy)\text{-}(bpy)H_2O]^{2+}$ (0.01 mM), Co(III) (20 mM), and 4-methoxythioanisole (10 mM), the catalytic photooxidation of sulfide produced much fewer TONs (only 101 after 8 hours). This indicates that as compared to a multicomponent system, the supramolecular structure has better photocatalytic activity. Furthermore, control tests demonstrated that photooxidation of sulfide requires complicated, light, and sacrificial electron acceptors. Interestingly, after 8 hours of reaction, the Ru_{phot}−Ru_{cat}−H_2O system was supplemented with an extra 20 mM Co(III). The TON rose to about 1000 when the resultant solution was exposed to radiation for an additional 4 hours. This illustrates the catalyst's high photostability. For one hour, monochromatized light of λ = 450 nm (strength of light is $60.0 mWcm^{-2}s^{-1}$) was used to irradiate phosphate buffer (0.1 M, 5 mL, pH 6.8) including complex 3 (0.01 mM), Co(III) (20.00 mM), and 4-methoxythioanisole (10.00 mM) and get TON of 60. The apparent quantum yield, as resolute by tracking the product's production using H NMR spectroscopy, was 0.7%. The range of photocatalytic activity of these complexes was further investigated using various substrates. The superior performance of substrates with electron-donating groups over those with electron-withdrawing groups suggests that there may have been an electrical influence. Both Ru_{phot}−Ru_{cat}−H_2O and Ru_{phot}−Ru_{cat}−Cl catalysts could photooxidize a sulfide with a $-NH_2$ substituent at a greater TON than a sulfide with a $-NO_2$ group (22).

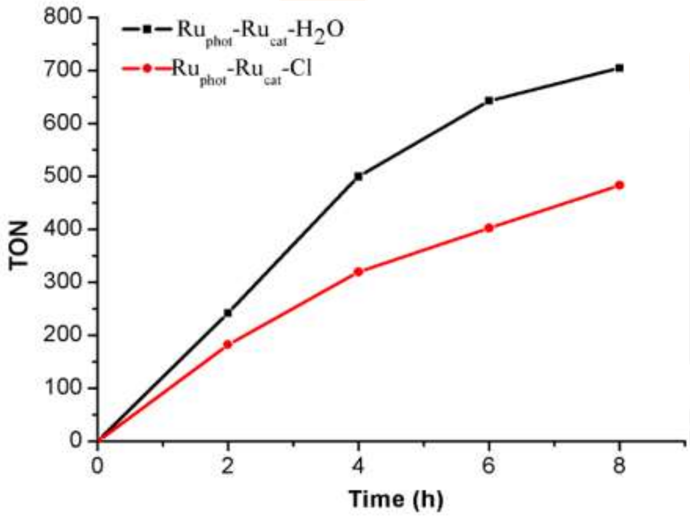

Figure 3. Turnover number for 4-methoxythioanisole photocatalytic oxidation by 2 (red) and 3 (black) under argon as a function of exposure duration (23).

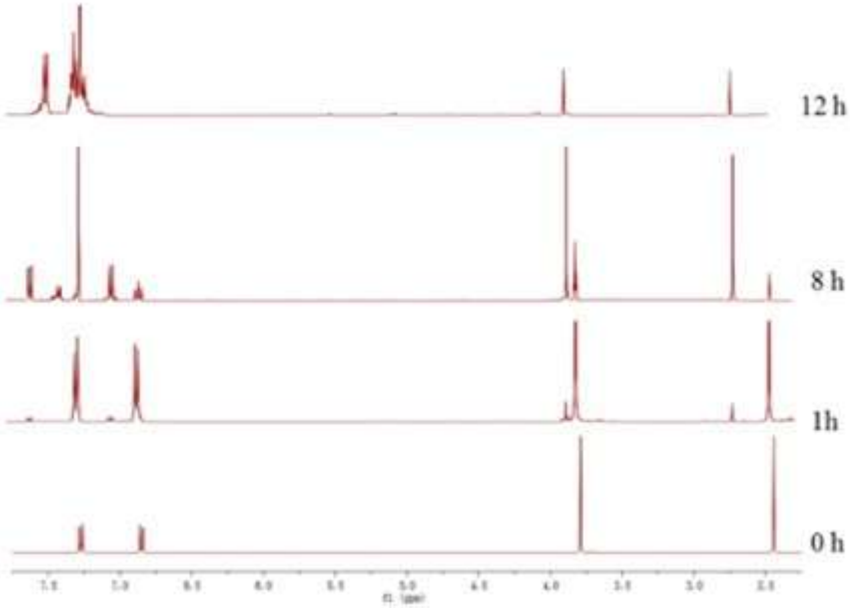

Figure 4. Using 3 as the photocatalyst in the photooxidation process, the H NMR ($CDCl_3$) spectra of the product and substrate (4-methoxythioanisole) at various reaction times (24).

2.6 Examples of Ru (III) complexes with high catalytic activity

The aryl–aryl coupling process has been catalyzed by the novel complexes. The reaction between phenylmagnesium bromide and bromobenzene, which produces biphenyl (Eq. 8), is the system selected for our investigation. The analogous Grignard reagent was initially produced from bromobenzene. The aforesaid reagent was heated under reflux for 6 h, after which bromobenzene and complex selected for study were added. Biphenyl was produced by the reaction mixture following work-up.

(8)

When the catalyst is not used, just a very little quantity of biphenyl (1.4%) is produced. This quantity is insignificant in comparison to the yield of biphenyl produced by ruthenium complex-catalyzed processes. Many experiments with varying mole ratios of phenylmagnesium bromide as well as $[RuCl(PPh_3)_2(Sal\text{-}bh)]$ have been conducted to determine the ideal amount of catalyst $[RuCl(PPh_3)_2(Sal\text{-}bh)]$ needed for coupling of phenylmagnesium bromide through bromobenzene. The outcomes are shown in Table 3. The Grignard reagent to ruthenium complex mole ratio, as determined by this experiment, was 100:1. This aligns with current finding. Biphenyl yields from reactions mediated by ruthenium(III) complexes are contingent on catalysts' efficacy, that closely linked to its capacity to produce active species (A) (25).

Ruthenium complexes containing PPh_3 or $AsPh_3$ catalyzed coupling processes that produced almost equal amounts of biphenyl, suggesting that none of these metals participated in the catalytic cycle. Table 4 displays results based on the aforementioned findings, the system shown in Figure 5 suggests a feasible pathway for coupling of phenylmagnesium bromide by bromobenzene, that is catalyzed with ruthenium(III) complexes. It was shown that ruthenium(III) complexes catalyze a similar process for linking phenylmagnesium bromide via bromobenzene (26). Evidence from the literature suggests that ruthenium-aryl intermediates (B and C) may exist (27). The complex was not used in the process; instead, ruthenium trichloride was used. The ruthenium trichloride-catalyzed reaction yields less than half as much biphenyl as the ruthenium(III) complex-catalyzed reactions. This suggests that, in comparison to the complexes, ruthenium trichloride has less catalytic activity (28).

Table 3. Biphenyl yields for ruthenium(III) complexes and phenylmagnesium bromide with varying mole ratios (29).

S.no	$[RuCl(PPh_3)_2(Sal\text{-}bh)]$ (mol)	Yield (%)	Phenylmagnesium bromide (mol)
1	0.00003	10.5	0.005
2	0.00004	13.4	0.005
3	0.00005	16.2	0.005

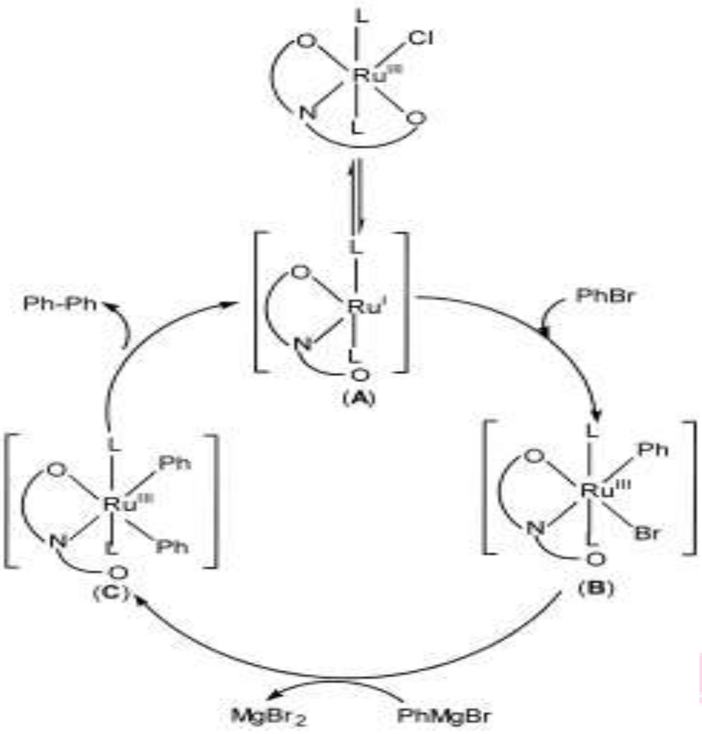

Figure 5. A plausible explanation for how ruthenium(III) complexes accelerate Phenylmagnesium bromide and bromobenzene coupling (Jayabalakrishnan et al., 2003).

Table 4: Ruthenium(III) Schiff base complexes as catalyst for biphenyl yields (30).

Complex	Yield of biphenyl	
	(in g)	(%)
(1)	0.260	16.2
(3)	0.210	13.6
(5)	0.240	15.6

In the context ,"complex" likely refers to metal-ligand complexes used as catalysts in a chemical reaction to produce biphenyl. In catalytic studies, complexes are often numbered (e.g., Complex (1), Complex (3), Complex (5)) to distinguish between different catalysts with varied metal centers, ligand environments, or structural configurations. Complex (1) could be a Ruthenium(III) or Palladium(II) Schiff base complex with a specific ligand structure. Complex (3) and Complex (5) might represent similar metal complexes but with variations in the ligands or metal oxidation states.

3. CATALYTIC EFFICIENCY: PALLADIUM(II) COMPLEXES

3.1 Coordination geometry and redox properties

Palladium (II) complexes are known for their high catalytic effectiveness, which is mostly attributable to their advantageous redox characteristics and stable coordination geometry. Palladium takes on a square planar shape in majority of Pd(II) Schiff base complexes, which offers the best configuration for catalysis, especially in carbon-carbon coupling processes. By effectively overlapping the d-orbitals with the ligands' π and σ orbitals, this shape stabilizes the Pd(II) core and makes interactions with substrates easier.

The catalytic cycles of palladium (II) complexes are significantly influenced by redox characteristics. Pd(II) can enter oxidative addition and reductive elimination stages that are essential in cross-coupling reactions, although it is comparatively stable and does not experience as many redox shifts as ruthenium. Pd(II) is momentarily oxidized to Pd(IV) during oxidative addition, that enables it to establish bonds with substrates such as organic halides. In reactions where the complex creates carbon-carbon or carbon-heteroatom bonds, such as Suzuki, Heck, and Sonogashira couplings, this transition is crucial. These redox capabilities combined with square planar shape make Pd(II) complexes especially effective. The redox characteristics enable Pd(II) to easily engage in multi-step reactions with a high turnover rate, resulting in increased catalytic efficiency in organic synthesis, while the stable shape offers a strong framework for catalyst recycling.

Using cyclic voltammetry, redox chemistry of complexes 2-4 was investigated. A second reaction about +1.2 V shows twice the current as well as considerable chemical reversibility follows irreversible anodic event at +0.8 V in cyclic voltammograms of 2 (Fig. 7a). The three and four cyclic voltammograms show the same behaviors. The idea processes begin with free bromide ions in solution created when the bromo ligands separate or are replaced was one to consider. But according to Allen et al. (2005), the Br/Br 3 pair exhibits enhanced potential at +1.15 V that of first process.

According to Eq. (9), the oxidation of $[PdBr_2(C\text{-}NHC)_2]$ center must thus be linked to first step. Eq. (10), which describes decomposition of $[PdBr_2(C\text{-}NHC)_2]^{+}$ during electrochemical timeframe ($\sim 1ms$), would explain oxidation's observed irreversibility. Anodic current comparisons for two successive oxidation processes indicate that the breakdown product of two-electron oxidation $[PdBr_2(C\text{-}NHC)_2]^{+}$ center must be the cause of the second oxidation pair, albeit its origin cannot be determined with confidence. The structure complex is shown in figure 6 (Berben et al., 2011).

$$[PdBr_2(C\text{-}NHC)_2](2) \longrightarrow [PdBr_2(C\text{-}NHC)_2]^{+}+e^{-} \qquad (9)$$

$$[PdBr_2(C\text{-}NHC)_2]^{+} \rightarrow decompositionproduct(s) \qquad (10)$$

In complex 3's cyclic voltammogram, the distinctive anodic peak at 1.1 V is produced by pair-electron proton-coupled oxidation of respectively of two hydroquinone substituents (Figure 7b), which is combined with the anodic processes previously outlined to create an overall broad peak (31). The process's anodic current is completely in line with interpretation (for $[complex] = 2.0mM$, anodic peak current of 3 is 17 μA, while that of 2 is 7 μA, meaning that 2's anodic peak current is 2.4 μA/e- or 3e- in total, while 3's is 7e- in total). When reducing a protonated quinone species, a minor cathodic peak at +0.26 V is often seen in return sweep $[PdBr_2(C\text{-}NHC\text{-}q/H^{+})_2]^{2+}$ in Eq. (11)). The forward sweep creates Complex 4, which has the same oxidative processes as 2 and 3. As previously noted, it is allocated as such (Fig. 7c). However, the decrease process at 0.2 V and the wide process at about -0.6 V are more intriguing (Berben et al., 2011).

$$[PdBr_2(C\text{-}NHC\text{-}hqH_2)_2](3) \rightleftarrows [PdBr_2(C\text{-}NHC\text{-}q/H^{+})_2]^{2+}+4e^{-}+2H^{+} \qquad (11)$$

Switching experiments demonstrate that the -0.2 V process generates a peak of +0.3 V in the reverse scan and is only weakly reversible. They discovered that the cyclic voltammetry is entirely consistent with what has been seen for reactive quinones before (32), (33). The initial reduction is related by the radical anion pair of benzoquinones and semiquinone, as shown in Eq. (12). Weak chemical reversibility indicates a process that consumes semiquinone anion in electrochemical period (ca. 1 ms). It has been demonstrated before that pendant semiquinone radical anions may bind to metal center, particularly with dislodging halogen co-ligands. Furthermore, we have seen ligand dissociation events brought on by internal electron transfer between a metal center and semiquinone or hydroquinonyl substituents (34). As an alternative, benzoquinone and hydroquinone anions (hqH^{-}) may be produced disproportionately by the readily removed proton from solvent-electrolyte medium by reactive semiquinone radical anions (35),(36),(37). The low reversibility and reduced current for semiquinone anion combination at 0.6 V (Eq. (13)) may be explained by such mechanisms. The semiquinone/hydroquinone dianion pair needs to be swept over to avoid anodic peak at +0.3 V (see Fig. 7d, inset). The oxidation of types through a corresponding or protonated hydroquinone group (s) must thus be the cause of +0.3 V anodic peak, independent of the chemical process that occurs before the semiquinone radical forms (38).

$$[PdBr_2(C\text{-}NHC\text{-}q)_2](4)+2e^{-} \rightleftarrows [PdBr_2(C\text{-}NHC\text{-}sq^{\cdot-})_2]^{2-} \qquad (12)$$

$$[PdBr_2(C\text{-}NHC\text{-}sq^{\cdot-})_2]^{2-}+2e^{-} \rightleftarrows [PdBr_2(C\text{-}NHC\text{-}hq^{2-})_2]^{4-} \qquad (13)$$

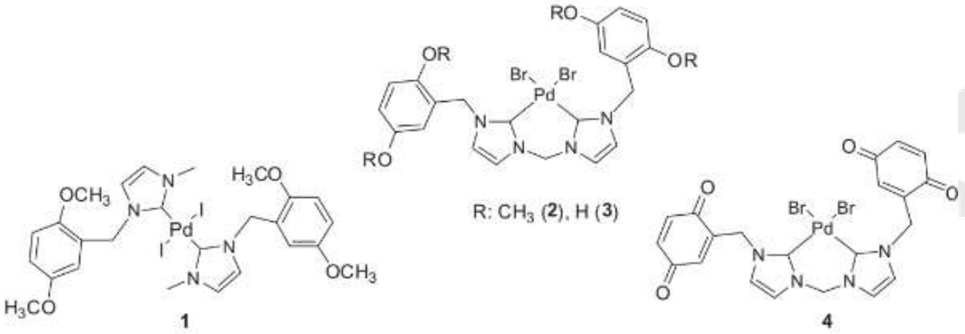

Figure 6. Electrochemically active (hydro)quinonyl substituents in novel (NHC)$_2$Pd(II) complexes (39).

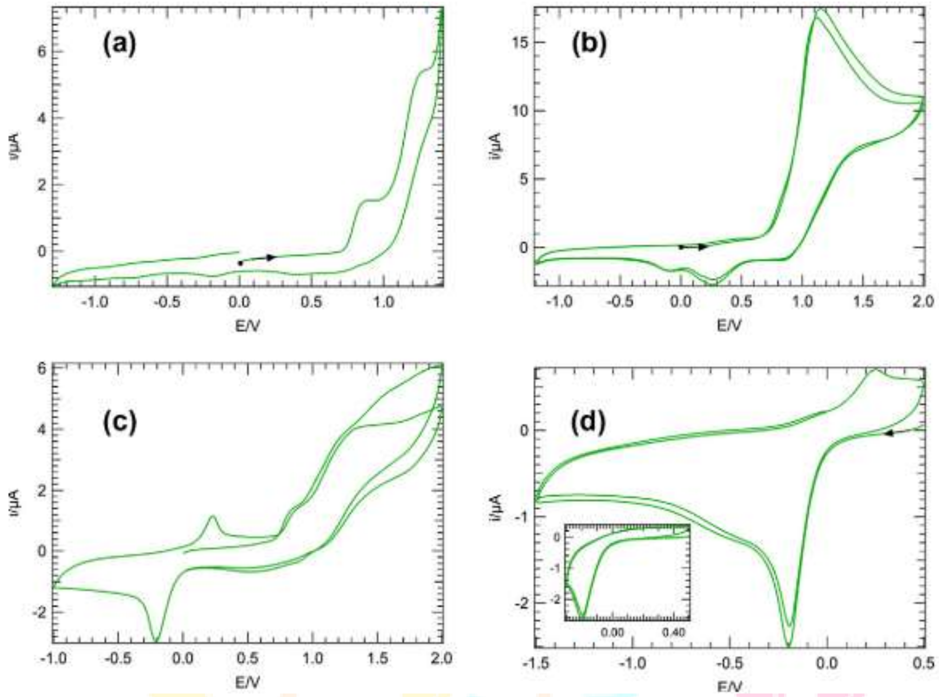

Figure 7. Cyclic voltammograms of complexes (a) 2, (b) 3, and (c and d) 4. Conditions: solvent = acetonitrile – 0.1$molL^{-1}$[$NBu^n{}_4$][PF_6]; [complex] = 2.0 mmol L1; working electrode = freshly polished 0.5 mm diameter glassy carbon-disc; scan rate = 100mVs^{-1} ; temperature = 295 K; $E_{1/2}$ (ferrocenium-ferrocene) = 0.47 V. Note the current scales differ in (a)–(d) (40).

3.2 Moderate TOFs and TONs

$[Pd_2(dppf)_2(SC_{12}H_8S)]_2(OTf)_4$ (Figure 7) for Suzuki-Miyaura reaction by eagerly available $Co_2(CO)_8$ as C1 source. It is noteworthy Pd(II) complexes of aryldithiolate $[Pd_2(P^{\cap}P)_2\{S(C_6H_4)nS\}]_2(OTf)_4$ (n=1 or 2; $P^{\cap}P=dppe$, $dppf$ and Xantphos) displayed outstanding catalytic activity in SuzukiMiyaura (41) ,(42) and Heck C-C (43) cross-coupling reactions.

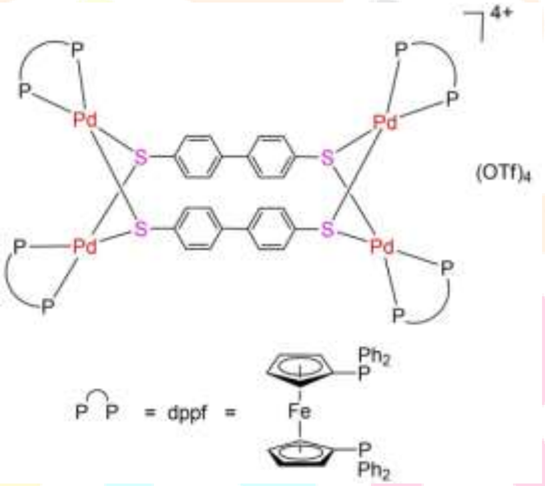

Figure 7. The palladium complex $[Pd_2(P^{\cap}P)_2\{S(C_6H_4)nS\}]_2(OTf)_4$ used as catalyst in carbonylative Suzuki-Miyaura reaction (44).

The concentration of the catalyst is a crucial factor in assessing the protocol's viability for large-scale implementation. For synthesis of biaryl ketones, the conducted experiments to investigate catalyst loading. To establish a range of palladium solution concentrations of 1 mol%, 10^{-1} mol%, 10^{-2} mol%, 10^{-3} mol%, as well as 10^{-4} mol%, First dissolved a catalyst in acetonitrile as a solvent. In this instance, the carbonylative Suzuki-Miyaura using Iodobenzene (1a) as well as phenylboronic acid (2a) synthesis of benzophenone (3a) (Table 5). Up to 10^{-3} mol% of palladium concentration was largest amount of iodobenzene that could be converted, and maximum yield of benzophenone (93%) was achieved at 80°C for 12 h. The range of TON generated was between $94 and 9.4 \times 10^4$, while the range of TOF was between 7.8 and 7.7×10^3 (Table 5, entry 1-4).

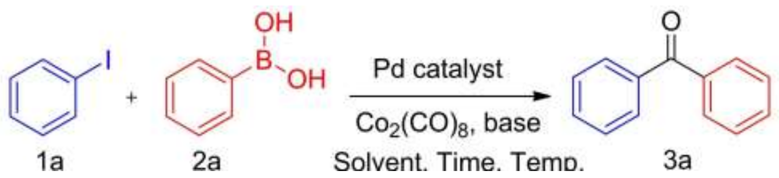

(14)

$Co_2(CO)_8$ (0.3 mmol), 1a (0.5 mmol), 2a (0.7 mmol),K_2CO_3 (2 equiv), solvent (4 mL), and 80°C for 12 hours are the reaction conditions. b, c, and yield ascertained with GC-GCMS, d 100° C for 18 hours, as indicated by Eq. (14) (45).

Table 5: Catalyst loading's impact on reaction[a]

Entry number	Pd (1) mol (%)	Conversion (%)	synthesis of benzophenone (%)	TON	TOF ($h^{-1)}$
$9.4 \times 10^1 0.78 \times 10^1 1$	1	96	94		
$9.4 \times 10^2 7.8 \times 10^1 2$	0.1	96	94		
$9.3 \times 10^3 7.7 \times 10^2 3$	0.01	96	93		
$9.3 \times 10^4 7.7 \times 10^3 4$	0.001	95	93		

With the optimum reaction conditions currently in place, the variety of biaryl ketone might be produced using the technique that was created (Table 5). In a smooth reaction with phenylboronic acid (2a), simple iodobenzene (1a) produced benzophenone (3a) with a high yield of 9.3×10^4 TON as well as 7.7×10^3 TOF (Table 6, entry 4). Then looked at how well the substituted aryl iodide by phenylboronic acid may function under ideal reaction conditions. The aryl iodide's electron-donating functions are effectively converted into the intended product.

Phenylboronic acid reacts with electron-donating groups like p-Me and p-OMe to produce high yields of 3b and 3c; nevertheless, the range of TON and TOF is 8.9×10^4 to $9.2 \times 10^4$and7.4×10^3to7.6×10^3, respectively (Table 6, entries 1 and 2). Acid-sensitive groups, such as p and o amino iodobenzene, were also used for this reaction. Interestingly, the reactions produced good yields of 3d and 3e with greater TOF and tolerated functional groups (7.2×10^3 and 6.6×10^3) and TON (8.7×10^4 and 8×10^4) (Table 6, entries 3 and 4). In Eq. (15), the palladium catalyst for biaryl ketone synthesis is identified.

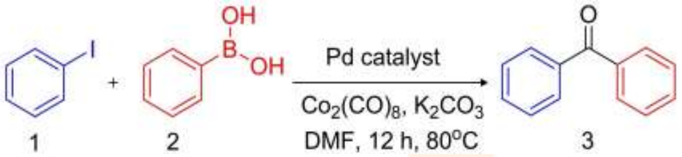

(15)

Table 6. Palladium catalyst's range for biaryl ketone synthesis carbonylative Suzuki-Miyaura using Iodobenzene (1) and phenylboronic acid (2) produced benzophenone (3)(46).

Entry no	1	2	3	TON	TOF (h^{-1})
1	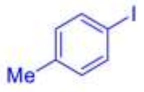 1b 1-iodo-2-methylbenzene.	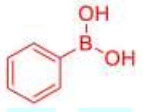 2a phenylboronic acid	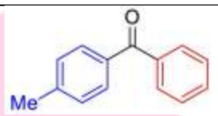 3b/89 1-phenyl-2-methyl-1-propanone	8.9×10^4	7.4×10^3
2	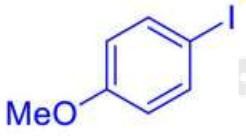 1c 1-iodo-2-methoxybenzene	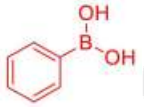 2a phenylboronic acid	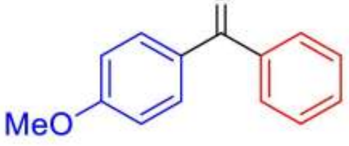 3c/92 1-phenyl-2-methoxy-1-propanone.	9.2×10^4	7.6×10^3
3	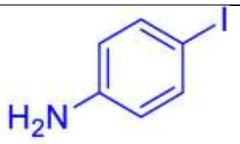 1d 2-iodoaniline	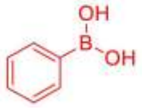 2a phenylboronic acid	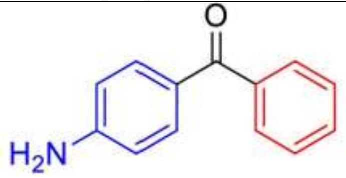 3d/87 1-phenyl-2-amino-1-	8.7×10^4	7.2×10^3

			propanone		
4	 1e 2-iodoaniline.	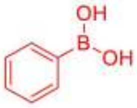 2a phenylboronic acid	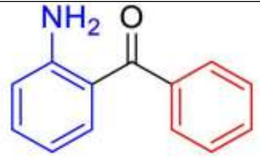 3e/80 1-phenyl-2-amino-1-propanone	8x10^4	6.6 x10^3
5	 1f 2-iodo-1-bromobenzene.	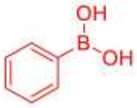 2a phenylboronic acid	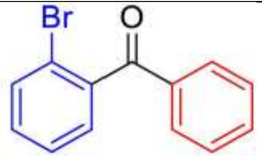 3f/80 1-phenyl-2-bromo-1-propanone	8.4x10^4	6.6 x10^3

3.3 Selective oxidation of alkenes and alkynes

3.3.1 oxidation of alkenes

When coupled to a palladium(II) salt, an alkene that is typically electron-rich 2 becomes noticeably more electrophilic (Figure 8). Because of this, oxygen nucleophiles like water, alcohols, or acetate ions can attack it. To create α-allyl complex 3 (Path 1), a typical approach entails the nucleophile (or a base) initially abstracting an allylic proton. To produce allylic oxidation products 4 and 5 as well as palladium(0) species that could reoxidized to palladium(II) to complete catalytic cycle, this extremely stable complex can next go through nucleophilic substitution reaction, frequently by external sphere method. The nucleophile attacks activated alkene 2 directly via alternative chemical routes, resulting in -alkylpalladium intermediate 6a (and/or its regioisomer 6b) by coordinated nucleopalladation (47). Depending on its regioselectivity, α-hydride elimination (Path 2) can subsequently be applied to intermediate 6a to provide either product 4 of allylic oxidation or product 7 of vinylic oxidation. Water is often the nucleophile in the Wacker oxidation, and resulting enol 7 (Nu = OH) tautomerizes to provide aldehyde. However, note that palladium is thought to promote even this tautomerization (48).

In initial nucleopalladation procedure, pathway 2 is coupled with synthesis of regioisomer 6b to produce up to four dissimilar possible oxidation products. Re-oxidation to active Pd(II) types required to finish the cycle after -hydride elimination produces HPdX species that are easily eliminated by reductive elimination to expel HX. A third oxidation pathway uses an oxidizing agent or trapping reagent to further functionalize the -palladium intermediates 6a6b, forming new -bond at carbon where palladium is attached (Path 3). A 1,2-difunctionalization product 8 is the end outcome of this. Often, a Pd(II) species regenerates instantly via this last route, eliminating the need for further catalytic oxidation. Once more, quantity of isomeric products that can be generated depends on mechanism of succeeding oxidative functionalization as well as regioselectivity and stereoselectivity of the initial nucleopalladation process. It is clear from the three distinct paths covered above and illustrated in Figure 8 that a given reaction's mechanism is frequently not immediately apparent. Complicating matters further, given the reaction conditions, alkenes in products also starting materials may undergo isomerization. For example, two different chemical paths (Path 1 and Path 2) can provide the result of formal allylic oxidation by alkene transposition 4. This discusses the latest advancements in the three routes depicted in Figure 8 for Pd(II) catalyzed oxidation of alkenes, an emphasis intermolecular events involving the creation of new carbon-oxygen or carbon-nitrogen bonds (49).

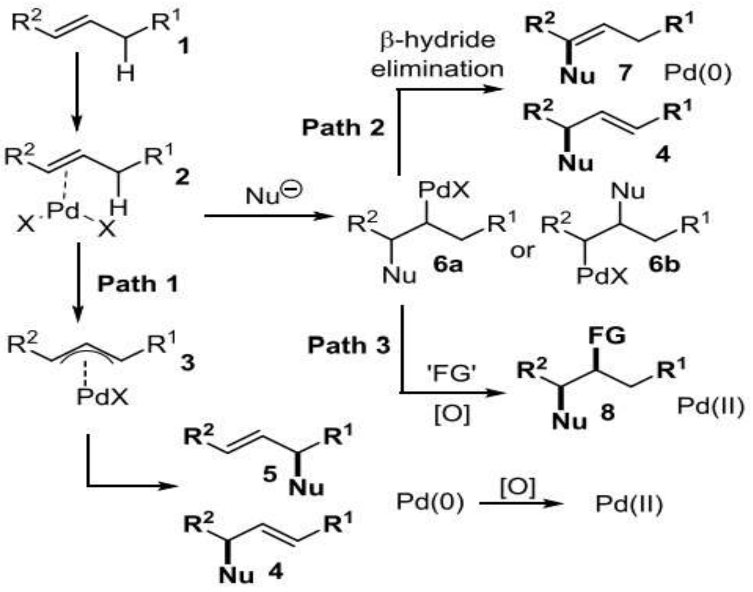

Figure 8: Alkene oxidation pathways accelerated by palladium (50).

3.3.2 Oxidation of Alkynes

The esters of arylpropiolic as well as alkylpropiolic acids were produced by oxidative carbonylations of terminal alkynes at ≡C–H bond (I), and because their great synthesis potential, they are of great theoretical and practical significance (51).

$$RC \equiv CH + CO + MeOH + Ox \rightarrow RC \equiv CC(O))Me + Red + 2H^{+} \qquad (16)$$

In this process, a variety of oxidizers (Ox) can be employed. According to eq. (16), the oxidizer reduction product in the specific instance of Ox = quinone is Red + 2H+ = hydroquinone (52).

Catalytic systems that are selective in comparison for Equation (16). The following reactions occur on the most efficient system, $PdCl_2$–$CuCl_2$– NaOAc, with 70% alkyne selectivity:

$$RC \equiv CH + CO + MeOH + 2NaOAc + 2CuCl_2 \underset{\rightarrow}{PdCl_2} RC \equiv CC(O)Me + 2NaCl + 2CuCl + 2AcOH \qquad (17)$$

Equation (17), which is autocatalytic, is part of this multifunctional catalytic system, as was previously discovered. The element that catalyzes the mechanism's step for the production of the palladium alkynyl complex is Cu(I) chloride, which is produced when $CuCl_2$ is reduced (18):

$$RC \equiv CH + CuCl\text{-}\vec{H}CLRC \equiv CCU \underset{\text{-}CuCl}{\overset{PdCl_2}{\rightarrow}} RC \equiv CPdClC\underset{\rightarrow}{O}RC \equiv CC(O)PdCl \underset{RC \equiv CC(O)OMe}{\overset{\overset{MeOH}{\rightarrow}}{\downarrow}} HPdCl2CuCl_2PdCl_2 + 2CuCl + HCl \qquad (18)$$

The Ag(I), Hg(II), and Cu(I) alkynyl complexes' production and reactivity assessments in Eq. (17), as well as kinetic investigations and the measurement of the kinetic isotope effect, validated the mechanism in Eq. (18). Additionally, these investigations enabled the execution of a novel catalytic process employing Cu(I), Cu(II) , and Pd(II) as catalysts and oxygen as the oxidant:

$$RC \equiv CH + CO + MeOH + 1/2O_2 PdCl_2, CuCl, \underset{\rightarrow}{CuCl_2}\ RC \equiv CCOOMe + H_2O \qquad (19)$$

The reaction in Eq. (19) can serve as a foundation for Since it doesn't create any acid, the small-scale production of alkynylcarboxylic acid esters eliminates the need for base to neutralize acid.

(1) Mechanisms involving key alkoxycarbonyl (methoxycarbonyl) intermediate in Eq. (20).

$$PdX_2 + MeOH + CO \underset{\text{-}HX}{\rightleftarrows} XPdC(O)OMeRC \equiv \underset{\rightarrow}{C}HXPC(R) = CHC(O)OMe\text{-}HP\vec{d}XRC \equiv CC(O)OMe \qquad (20)$$

(2) Creating a vital Pd(II) alkynyl complex is one of the mechanisms for electrophilic substitution of palladium (II) for hydrogen in alkyne in Eq. (21):

$$PdX_2 + RC \equiv CH \underset{\text{-}HX}{\rightleftarrows} XPdC \equiv CR\underset{\rightarrow}{C}OXPdC(O)C \equiv CR \underset{\text{-}HpdX}{\overset{MeOH}{\rightarrow}} RC \equiv CC(O)OMe \qquad (21)$$

There are no known second-group mechanisms. As shown above, palladium (II) does not form alkynyl complexes as easily as Cu(I) or Ag(I). Nevertheless, there are certain Pd(II) alkynyl complexes, thus it is not unreasonable to assume that electrophilic replacement of palladium for hydrogen atom in alkyne will not result in the creation of such a complex (53).

3. 4. Examples of Pd(II) complexes with notable catalytic activity

Brown and green complexes of compositions $[(L)_2Co]NO_3$, 1, as well as $[(L)_2Ni]$, 2 were produced by the separate reactions of two equivalents of 2-((2-(benzylthio)phenylimino)methyl)phenol, HL ligand with

$Co(NO_3)_3.6H_2O$andNi$(OAc)_2$-$4H_2O$ in methanol (Figure 9). Following a 1:1 mol interaction between the ligand HL and Pd(MeCN)2Cl2 in acetonitrile solution, complex $[(L)PdCl]$, 3 was created.

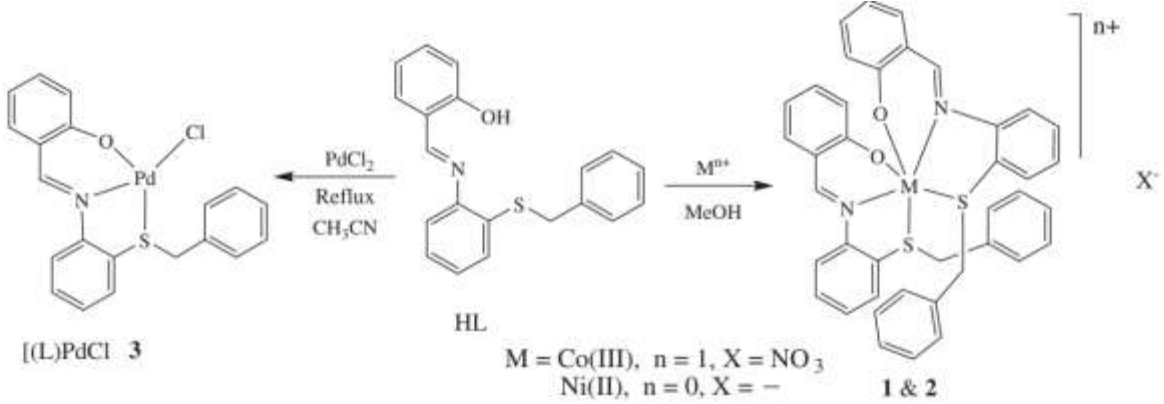

Figure 9: Synthesis of $[(L)_2M]^{n+}$ and $[(L)PdCl]$ (54).

The ligand binds metals in a tridentate (O, N, S) pattern over deprotonated phenolic-O, imine-N, as well as thioether-S atoms in all of the complexes to create two fused rings, one with six members and the other with five. For $[(L)_2Co]NO_3$, 1 to meet oxidation state of Co(III), one NO_3 ion is enough. Both the H NMR spectra and the microanalytical results support the complexes' structure (55).

- **Heck reaction**

Heck coupling is a significant C–C coupling reaction that is catalyzed by palladium and involves arylhalides (iodoaryls and bromoaryls) and styrene as substrates. In ambient conditions, investigate how $[(L)PdCl]$ catalyzes Heck coupling events. Using $[(L)PdCl]$ as a catalyst in refluxing methanol and with K_2CO_3, changes of arylhalides (Br and I) to consistent stilbene derivatives after reaction through styrene. Table 7 displays the outcomes of the transformation. Following the reaction, palladium catalyst was separated, as well as coupling reactions were seen when the separated catalyst was reused. While keeping the other conditions constant, the catalyst's reusability was tested up to three times for reaction. H NMR spectroscopy was used to characterize the products (57).

Table 7: Heck reaction with catalyst 3 (57).

Aryl Halide	Product	Isolated Yield (%)
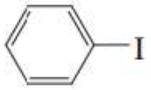 Iodobenzene	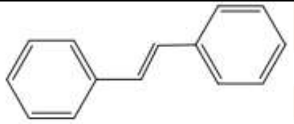 1,4-diphenyl-1,3-butadiene	95
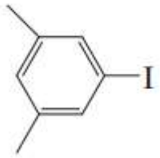 1-iodo-2,4-dimethylbenzene.	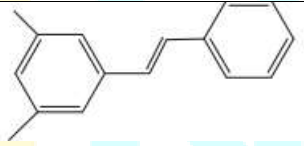 1,4-diphenyl-1,3-butadiene	92
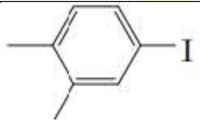 1-iodo-2,4-dimethylbenzene.	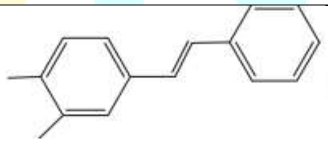 1,4-diphenyl-1,3-butadiene	92
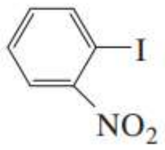 4-iodonitrobenzene.	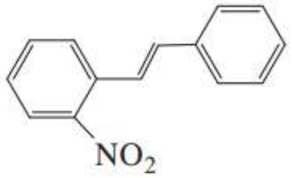 1,4-diphenyl-1,3-butadiene.	90
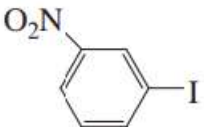 4-iodonitrobenzene.	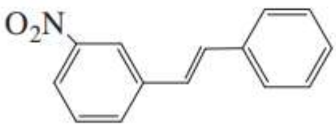 1,4-diphenyl-1,3-butadiene.	92

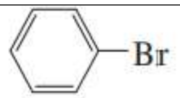 bromobenzene.	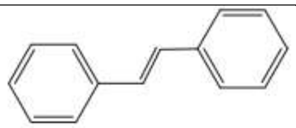 1,4-diphenyl-1,3-butadiene	82
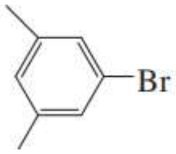 4-bromotoluene.	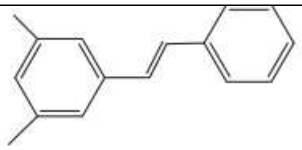 1,4-diphenyl-1,3-butadiene	80

Solvent = MeOH, base = K_2CO_3, time = 4 h.

4. COMPARATIVE ANALYSIS

4.1 Influence of Metal Center (Ru(III) vs. Pd(II))

The catalytic behavior of Schiff base complexes is pointedly influenced with metal center, with Ruthenium (III) and Palladium (II) demonstrating distinct reactivity patterns due to their unique redox properties, structural stability, and preferred geometries.

4.1.1 Redox Properties and Stability

- Ruthenium (III): Ru(III) is known for its versatility in redox chemistry, easily shifting between multiple oxidation states (commonly Ru(II) ↔ Ru(III) ↔ Ru(IV)), which enhances its efficiency in redox-based catalytic reactions such as oxidations. This multivalency allows Ru(III) to participate in rapid electron transfer, facilitating reactions like alcohol oxidations to aldehydes or ketones by high TOF and TON. Ru(III) complexes in Schiff bases can stabilize higher oxidation states and maintain-structural integrity, which contributes to prolonged catalytic cycles.
- Palladium (II): Pd(II) complexes, while not as redox-active as Ru(III), exhibit stable coordination primarily in Pd(II) with occasional transitions to Pd(IV) in specific catalytic cycles. This stability is particularly advantageous in carbon-carbon coupling reactions (e.g., Suzuki, Heck) where oxidative addition and reductive elimination steps are key. Unlike Ru(III), Pd(II) is less suited for continuous redox transitions but is highly effective in coupling reactions, where stability and structural geometry play a greater role than redox flexibility.

4.1.2 Structural Geometry

- Ru(III) Complexes: Ru(III) Schiff base complexes can adapt various geometries (octahedral or square planar, depending on ligands), allowing them to accommodate a broader range of substrates. This structural flexibility is beneficial in oxidation reactions as it provides better orbital overlap with the Schiff base ligands, thus enhancing catalytic efficiency and enabling diverse reaction pathways.
- Pd(II) Complexes: Pd(II) complexes generally maintain a square planar geometry, optimizing d-orbital overlap for stable interactions with ligands. This geometry is ideal for coupling reactions, where precise alignment aids in substrate coordination, ensuring high yields and selectivity in forming C-C and C-N bonds.

4.1.3 Catalytic Efficiency and Reaction Types

I. Ru(III): Ru(III)-Schiff base complexes are highly effective in oxidation reactions, such as converting alcohols to aldehydes and ketones, and in selective oxidations of alkenes and sulfides. The flexibility in Ru's oxidation states enables faster reaction rates and longer catalyst lifespans due to efficient redox cycling.

[1] Pd(II): Pd(II) is optimized for cross-coupling reactions. Its relatively stable Pd(II) state supports efficient oxidative addition and reductive elimination, essential steps in Suzuki, Heck, and Sonogashira reactions. Although Pd(II) complexes display moderate TOFs and TONs, they are reliable in organic synthesis where stable and consistent bond formations are needed.

4.1.4 Equation of Comparison (Example Catalytic Cycles):

[2] For Ru(III):

$$Ru(III)+Oxident \longrightarrow Ru(IV) \longrightarrow Product+Ru(III) \qquad (22)$$

This redox cycle illustrates how Ru(III) facilitates continuous oxidation reactions in Eq. (22). This cycle represents the oxidative addition and reductive elimination crucial in Pd-catalyzed coupling reactions.

[3] For Pd(II):

$$Pd(II)+R\text{-}X \rightarrow Pd(IV)\text{-}R\text{-}X \rightarrow Product+Pd(II) \qquad (23)$$

This cycle represents the oxidative addition and reductive elimination crucial in Pd-catalyzed coupling reactions in Eq. (23).

Ru(III) is more suited for redox-intensive oxidation reactions, whereas Pd(II) is ideal for coupling reactions. These differences in metal centers significantly influence the types of reactions each metal can efficiently catalyze and their applications in organic synthesis.

4.2 Effect of Schiff base ligand structure and coordination geometry

The structure of Schiff base ligands significantly impacts the catalytic behavior of Ruthenium (III) complexes by influencing their stability, redox properties, and geometric configuration. Key structural aspects of Schiff base ligands, such as the donor atoms, flexibility, and steric effects, are central to optimizing Ru(III) catalytic efficiency.

4.2.1 Influence of Donor Atoms and Ligand Field Strength

Schiff base ligands with N_2O_2 donor sets (two nitrogen and two oxygen atoms) are commonly used with Ru(III) because they create a balanced ligand field that stabilizes various oxidation states of Ru. This stability enhances Ru(III) complex's catalytic efficiency in redox reactions by supporting reversible oxidation states (e.g., Ru(III) ↔ Ru(IV) transitions).

- **Electron Donating Effects**: Ligands with strong electron-donating groups, such as alkyl or methoxy substituents, can increase electron density around the Ru(III) center. This reduces the metal's oxidation potential, making it easier for Ru(III) to transition to higher oxidation states during catalytic cycles, which is beneficial in oxidation reactions.
- **Electron Withdrawing Effects**: Electron-withdrawing substituents, like nitro or halogens, create a more electrophilic metal center, which can help activate substrates, especially in reactions where the Ru(III) complex acts as an oxidizing agent.

4.2.2 Structural Flexibility and Coordination Geometry

The rigidity or flexibility of Schiff base ligand effects complex's geometry also metal's ability to adapt to different catalytic cycles the structure is shown in figure 10. For Ru(III), flexibility in the Schiff base ligand allows the complex to adjust to different coordination geometries, such as square planar or octahedral, which enhance the complex's reactivity by allowing it to accommodate various substrates (58).

- **Flexible Ligands**: Ligands with rotational freedom, such as those with aliphatic backbones, allow Ru(III) complexes to adopt geometries that optimize substrate binding and catalysis. This flexibility is advantageous in catalytic oxidation reactions, where adjusting geometry can improve access to substrates.
- **Rigid Ligands**: Rigid aromatic Schiff base ligands help maintain a stable square planar configuration around Ru(III), which enhances orbital overlap and stabilizes the metal-ligand interaction. This stability can improve the overall durability of the complex in catalysis and support higher turnover numbers (TONs) over extended cycles.

4.2.3 Steric Effects and Selectivity

Sterically demanding groups around Schiff base ligand can affect both accessibility of catalytic center and the selectivity of reactions.

- **Bulky Substituents**: Bulky groups on the ligand create a steric barrier around the Ru(III) center, which can protect it from undesirable side reactions and improve selectivity by controlling substrate access. For instance, sterically hindered Schiff base ligands can enhance selectivity in oxidation reactions, ensuring that only specific functional groups on substrates are oxidized.
- **Ligand Substitutions and Catalytic Reactivity**: By modifying the steric environment, certain substrates can be selectively activated or excluded, depending on the spatial arrangement around the Ru(III) center. This tailored accessibility is particularly useful in reactions requiring high substrate specificity, as it allows the complex to engage selectively with target molecules.

4.2.4 Redox Stability and Catalytic Longevity

The Schiff base ligand stabilizes Ru(III) across multiple redox states, which is essential for reactions requiring frequent electron transfers, like oxidations. Ligands with strong electron-donating or withdrawing groups can further stabilize intermediate oxidation states, preventing catalyst degradation and extending the lifetime of the complex. This stability under oxidative conditions allows Ru(III) Schiff base complexes to achieve high turnover numbers, making them efficient catalysts over prolonged reaction cycles.

In Ru(III) Schiff base complexes:

- **Donor atoms** in the ligand modulate electron density, affecting the metal's redox potential and catalytic efficiency.
- **Structural flexibility** allows for adjustable geometries, enhancing the complex's adaptability and reactivity.
- **Steric modifications** around the ligand improve selectivity and catalytic stability.
- **Redox stability** conferred by Schiff base ligands supports prolonged catalytic activity, crucial for industrial and synthetic applications where catalyst durability is essential.

Schiff base ligand structures are vital to maximizing the catalytic capabilities of Ru(III) complexes in selective oxidation and other redox-based applications (59).

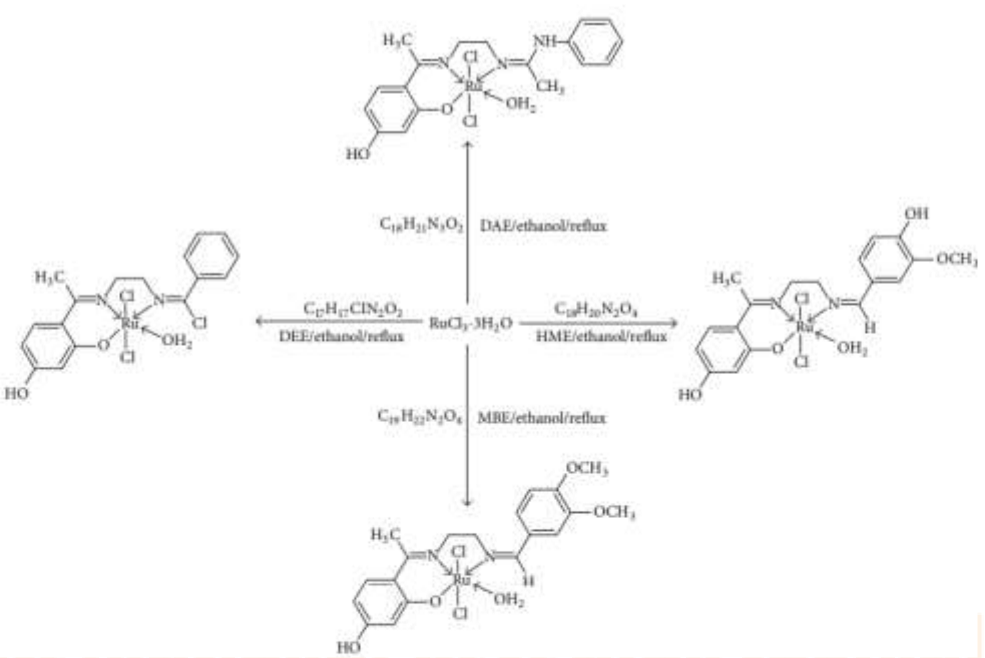

Figure 10: Structure of mononuclear ruthenium(III)-Schiff base complexes (60).

4.2.5 Coordination geometry of Ruthenium (III) complexes,

The coordination geometry of Ruthenium (III) complexes, particularly in ruthenium tetraammine and pentaammine systems, involves an octahedral environment with potential deviations due to specific ligand interactions (61). Key findings in the coordination geometry analysis of these complexes indicate that:

- **Primary Coordination Sphere**: Ruthenium (III) ions in these complexes are primarily coordinated by ammine ligands and occasionally by aqua (H_2O) or other monodentate ligands. For instance, complex trans-$[Ru(NH_3)_4(4\text{-pic})(H_2O)]^{3+}$ demonstrates a distorted octahedral geometry where the coordinated water molecule and a picoline (4-pic) ligand occupy axial positions, affecting the electronic distribution across the ruthenium center and subsequently influencing its reactivity.
- **Secondary Coordination Sphere**: Interactions involving hydrogen bonds among coordinated water molecule also solvent molecules or other hydrogen-bond donors in the environment play important role in determining coordination geometry and electronic properties. These interactions affect the energy levels of electronic orbitals through ligand-field and density functional theory (DFT) calculations, which show shifts in charge-transfer bands and changes in the g-tensor values observed in electron paramagnetic resonance (EPR) spectra.
- **Equations and Reactions**:

  One of the key reactions for Ruthenium (III) ammine complexes involves NO release, followed by coordination changes involving water in Eq. (24):

$$trans\text{-}[Ru^{II}(NO)(NH_3)_4(L)]^{3+} + red + H_2O \rightarrow trans\text{-}[Ru^{II}(NH_3)_4(L)(H_2O)]^{3+} + oxi + NO \qquad (24)$$

Ligand substitution reactions, such as halide (Cl^-, Br^-) replacing coordinated water, are also significant in characterizing these complexes shown in Eq. (25):

$$trans\text{-}[Ru(NH_3)_4(4\text{-}pic)(H_2O)]^{3+} + X^- \rightarrow trans\text{-}[Ru(NH_3)_4(4\text{-}pic)(X)]^{2+} + H_2O \qquad (25)$$

The determined pKa values and rate constants for water ligand substitution demonstrate the impact of axial ligands such as 4-picoline, which strengthen the Ru-OH_2 bond in the complex by increasing the ruthenium center's π-acidity. The stability and reactivity of ruthenium (III) complexes are impacted by primary and secondary contacts, which have a significant impact on the coordination sphere shape, according to these observations, which are corroborated by theoretical models (62).

4.3 Schiff base ligand structure and coordination geometry of Pd (II)

The structure of Schiff base ligands has important impact on catalytic efficiency, stability, also selectivity of Palladium (II) complexes. Key structural aspects of these ligands, such as their donor atoms, rigidity, and steric effects, play essential roles in determining the overall reactivity and durability of Pd(II) Schiff base complexes in catalysis, particularly in carbon-carbon coupling reactions (63).

4.3.1 Influence of Donor Atoms and Ligand Field Strength

Schiff base ligands with different donor atoms (N_2O_2, N_2S_2, or N_2O donor sets) influence the electron density around the Pd(II) center, affecting the stability and reactivity of the complex.

[4] Electron Donating Effects: Ligands with electron-donating groups (e.g., alkyl or methoxy) enhance the electron density on Pd(II), reducing the metal's oxidation potential. This effect can improve the efficiency of Pd(II) in oxidative addition steps, which are critical in coupling reactions. Electron-rich environments around Pd(II) generally enhance reactivity in cross-coupling reactions by stabilizing the active Pd(II) state required for catalysis.

[5] Electron Withdrawing Effects: Electron-withdrawing substituents (e.g., nitro or halogen groups) reduce electron density on Pd(II), making the metal center more electrophilic. This adjustment can enhance selectivity by activating certain types of substrates more effectively, especially in reactions where the Pd(II) center needs to interact with electron-rich organic partners.

4.3.2 Structural Rigidity and Coordination Geometry

The rigidity or flexibility of Schiff base ligand influences geometry of Pd(II) complex, which affects its catalytic performance and substrate compatibility.

- Rigid Ligands: Schiff base ligands with rigid aromatic backbones help stabilize the Pd(II) center in square planar geometry, that highly favorable for carbon-carbon coupling reactions. This geometry facilitates efficient overlap of d-orbitals with the ligand's π and σ orbitals, stabilizing the Pd(II) complex and improving the binding and transformation of substrates.
- Flexible Ligands: More flexible ligands allow for minor conformational adjustments around the Pd(II) center, which can be beneficial in reactions that require subtle changes in geometry, such as selective activation of substrates with varying steric demands. Flexible Schiff base ligands can also support Pd(II) complexes in binding bulky or sterically hindered substrates, enhancing the versatility of these catalysts in synthetic applications.

4.3.3 Steric Effects and Selectivity

Steric modifications in Schiff base ligands, such as adding bulky substituents around the coordination sphere, influence substrate accessibility to the Pd(II) center and help control reaction selectivity.

- Bulky Substituents: Steric bulk around the Schiff base ligand creates a shield around the Pd(II) center, which can prevent undesirable side reactions and increase selectivity by controlling which substrates can approach the catalytic center. This is particularly useful in coupling reactions, where selectivity in C-C or C-N bond formation is critical for complex molecule synthesis. For instance, bulky substituents can block smaller, non-target substrates, thereby improving selectivity for larger or more reactive partners.
- Ligand Tuning for Specific Reactions: By adjusting the steric environment of the ligand, Pd(II) complexes can be tailored for specific coupling reactions, such as Suzuki, Heck, or Sonogashira couplings. These reactions benefit from precise control over substrate access and catalytic cycle steps, especially when the catalyst is reused across multiple cycles.

4.3.4 Redox Stability and Catalytic Longevity

Schiff base ligands stabilize Pd(II) in a relatively narrow redox range, which is ideal for reactions requiring limited oxidative changes. Ligands that stabilize Pd(II) prevent the formation of Pd(0) aggregates, which can lead to catalyst deactivation in many cross-coupling reactions.

- Stabilization by Schiff Base Ligands: Strongly coordinating Schiff base ligands enhance the Pd(II) complex's resistance to reduction or degradation, thus improving its longevity in catalytic cycles. For instance, ligands with electron-donating or -withdrawing substituents can tune the redox potential to balance between oxidative addition and reductive elimination, essential for the efficiency of Pd(II)-catalyzed coupling reactions.

In Pd(II) Schiff base complexes:

- Donor atoms modulate the electron density around the Pd(II) center, impacting catalytic efficiency and selectivity in coupling reactions.
- Structural rigidity favors a stable square planar geometry, optimizing the complex for C-C and C-N bond-forming reactions.
- Steric effects enhance selectivity by controlling substrate access, improving efficiency in targeted coupling reactions.
- Redox stability provided by Schiff base ligands extends the catalyst's operational life, making Pd(II) Schiff base complexes reliable for high-yield synthesis.

The structure of Schiff base ligands is vital for maximizing catalytic performance of Pd(II) complexes, especially in applications requiring precise bond formation and selectivity, such as in pharmaceuticals and fine chemical synthesis (64).

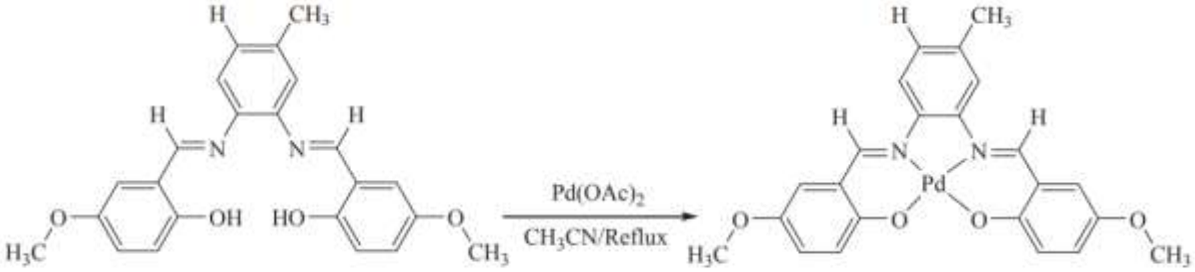

Figure 11. Synthesis of Pd(II) complex (65).

Reaction of $Pd(OAc)_2$ and H_2L in refluxing acetonitrile, afforded neutral palladium(II) complex. Figure 11 illustrates how the Schiff base ligand's Pd(II) complex was made.

The neutral palladium (II) complex was produced via reaction of $Pd(OAc)_2$ with H_2L in refluxing acetonitrile. Figure 11 illustrates how Pd(II) complex of Schiff base ligand was made.

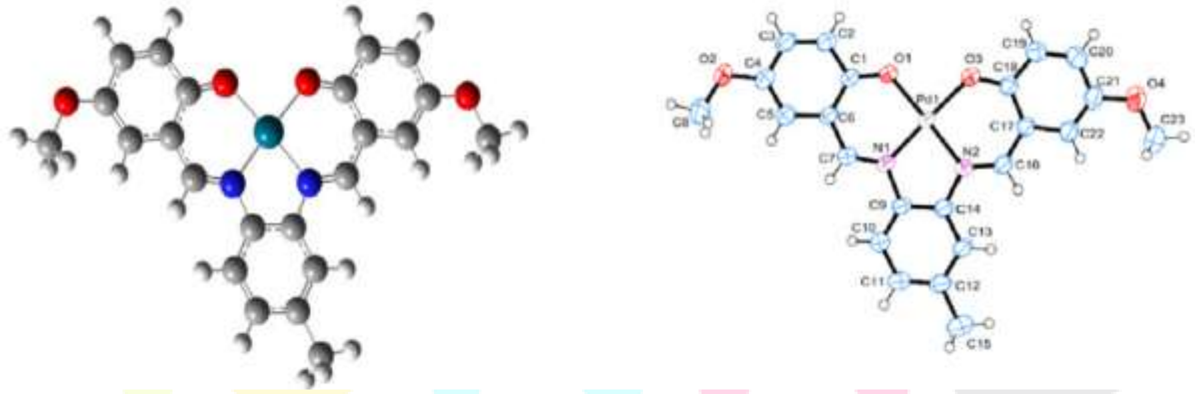

Figure 12. Optimized and X-ray crystal structures of PdL by labeling atoms (66).

Figure 12 displays the complex's molecular structure. Table 8 offers list of selected bond lengths and angles. The Pd(II) complex (Figure 12) kept in distorted square planar direction with diagonal angles $N1\text{-}Pd1\text{-}O3$ (178.17) and $N2\text{-}Pd1\text{-}O1$ (177.34) around the palladium atom, as well as two Ne as well as two O-atoms in cis configuration. ($Pd1\text{-}O1$), ($Pd1\text{-}O3$), ($Pd1\text{-}N1$), and ($Pd1\text{-}N2$) have bond lengths of 1.982 Å, 1.989 Å, 1.953 Å, and 1.955 Å, respectively. PdeO and PdeN distances are within the published limits, as well as single crystal X-ray diffraction exhibited palladium metal core of complex is surrounded by a somewhat distorted square-planar geometry. The main geometric distinction between the ligand as well as complex is angle formed by two oxygen-connected benzene ring planes. This angle was measured using fake atoms. These fake atoms have an angle of 180° in the complex, and the ligand has an angle of almost 110°. As a result, all three benzene rings are located in same plane during complexation. While phenolic C-O and C-C bond lengths between the imine unit and phenyl ring drop when the phenolic OH group deprotonates, C=N bond length in imine group increases when coordinated to metal center (Table 8). According to calculations and tests, Pd-O bond length in Pd(II) complex extended (Table 8) (67).

Table 8: Comparison of the determined and chosen experimental bond lengths [Å] as well as angles [∘] for [Pd($C_{23}H_{20}N_2O_4$)] and $C_{23}H_{22}N_2O_4$ (68).

	Pd(II) complex	
	Experimental	**Calculated**
Bond length (Å)		
$N1\text{-}C9$	1.421	1.414
$N1\text{-}C7$	1.301	1.297
$N2\text{-}C14$	1.424	1.413
$N2\text{-}C16$	1.293	1.298
$O1\text{-}C1$	1.301	1.280
$O3\text{-}C18$	1.301	1.280
$C6\text{-}C7$	1.426	1.417
$C16\text{-}C17$	1.415	1.416
$Pd\text{-}O1$	1.982	2.011
$Pd\text{-}O3$	1.989	2.013
$Pd\text{-}N1$	1.953	1.987
$Pd\text{-}N2$	1.955	1.988
∘)**Bond angle (**		
$O3\text{-}Pd\text{-}N2$	95.08	93.51
$N1\text{-}Pd\text{-}O1$	94.47	93.56
$N1\text{-}Pd\text{-}N2$	83.28	83.29
$O1\text{-}Pd\text{-}O3$	87.18	89.62
$N1\text{-}Pd\text{-}O3$	178.17	176.81
$O1\text{-}Pd\text{-}N2$	177.44	176.85

The coordination geometry

The coordination geometry of Palladium (II) complexes often adopts a square planar geometry due to the d^8 electron configuration, which minimizes repulsions by forming a planar arrangement. In the case of Schiff base complexes with ONNO-type ligands, Palladium (II) can form stable, square planar coordination. The Pd(II) center coordinates with nitrogen as well as oxygen donors from ligand, creating a nearly ideal square planar structure with minimal distortions.

For instance, the Palladium Schiff base complex (PdL) coordinates with the nitrogen as well as oxygen atoms of tetradentate Schiff base ligand. The Pd–N and Pd–O bonds are typically shorter due to strong coordination. In this square planar arrangement, the Schiff base ligand stabilizes the complex, preventing changes in geometry, which might otherwise lead to higher coordination numbers in other metal center.

4.3.5 Example Equation for a Pd(II) Complex Formation

A ligand H_2L (where H_2L is a tetradentate Schiff base) and $Pd(OAc)_2$ undergo this reaction, which is followed by production of Pd(II) Schiff base complex in Eq. (26):

$$H_2L+Pd(OAc)_2 \longrightarrow PdL+2HOA_c \qquad (26)$$

In this equation, the Schiff base ligand H_2L and palladium acetate combine to form a Pd(II) complex with a square planar shape and release acetic acid. Under argon gas, this reaction is generally carried out in combination of organic solvents, such as methanol as well as chloroform, as well as light heating may be used to promote complexation (69).

4.4 Oxidation State and Redox Potential

Ruthenium (III)

[6] Oxidation States: Ru(III) is highly versatile and commonly exists in oxidation states ranging from +2 to +4, allowing it to participate effectively in redox processes. This flexibility enables Ru(III) complexes to shift between oxidation states (e.g., Ru(III) ↔ Ru(IV)) during catalytic cycles, particularly in oxidation reactions.

[7] Redox Potential: Ru(III) Schiff base complexes have redox potentials that support quasi-reversible redox cycles, which is advantageous in oxidation reactions where rapid electron transfer is needed. This quasi-reversibility is evident in the cyclic voltammetry data, showing a typical peak separation (150–400 mV) that indicates moderate electron transfer rates. The ability of Ru(III) to participate in

successive oxidation cycles with minimal degradation makes it an efficient catalyst for alcohol, alkene, and sulfide oxidation reactions.

[8] Catalytic Implication: The redox-active nature of Ru(III) makes it highly suitable for redox-based catalysis, where multiple electron transfers are required. For example, in oxidation reactions, Ru(III) Schiff base complexes can form high-valent Ru=O species, which actively participate in oxidation processes before returning to the Ru(III) state. This characteristic enhances catalytic turnover frequencies (TOFs) and turnover numbers (TONs), making Ru(III) Schiff base complexes especially effective in oxidation applications.

Palladium (II)

- Oxidation States: Palladium is typically stable in the +2 oxidation state but can transition to Pd(IV) under specific catalytic conditions, especially in oxidative addition steps during carbon-carbon coupling reactions (e.g., Suzuki, Heck). This transition is critical for reactions that require the formation and breaking of Pd-C bonds.
- Redox Potential: Pd(II) complexes generally exhibit lower redox flexibility than Ru(III) complexes. The redox potential of Pd(II) is suited to oxidative addition and reductive elimination steps rather than continuous redox cycling. As a result, Pd(II) complexes maintain structural stability, allowing efficient coupling of organic substrates in reactions like cross-coupling. This limited redox range is sufficient for reactions where Pd(II) undergoes temporary oxidation to Pd(IV), facilitating creation of C-C and C-N bonds.
- Catalytic Implication: Due to its stable redox behaviour, Pd (II) is less effective in reactions requiring frequent electron transfer but is highly efficient in coupling reactions where stability in the +2 state is beneficial. The Pd (II) centre's reactivity in oxidative addition and reductive elimination enables it to form stable intermediates in cross-coupling reactions, which are essential for forming complex organic compounds.

Ru(III): With high redox flexibility, Ru(III) Schiff base complexes are optimized for oxidation reactions. Its ability to undergo reversible redox changes contributes to high catalytic efficiency and durability in redox-intensive processes. Pd(II): Pd(II) complexes have a stable +2 state with limited transitions to Pd(IV). This stability supports their effectiveness in coupling reactions, where oxidative addition and reductive elimination are critical. The differences in oxidation states and redox potentials between Ru (III) and Pd (II) highlight their complementary roles in catalysis, with Ru (III) favouring oxidation processes and Pd (II) excelling in coupling reactions.

4.5 Reaction Conditions: Temperature, Solvent, and Substrate

Ruthenium (III)

- Temperature: Ru(III) Schiff base complexes are typically effective at moderate to high temperatures (50–100°C), which supports the redox cycles essential in oxidation reactions. Elevated temperatures accelerate redox transitions between Ru(III) and Ru(IV), increasing the catalytic rate and improving turnover frequencies (TOFs) and turnover numbers (TONs). However, extremely high temperatures can lead to catalyst decomposition, so maintaining a controlled reaction environment is crucial.
- Solvent: Polar, aprotic solvents such as dichloromethane (CH_2Cl_2), acetonitrile (CH_3CN), and dimethyl sulfoxide (DMSO) are commonly used with Ru(III) complexes. These solvents stabilize intermediate oxidation states and facilitate electron transfer. The use of oxidants, like N-methylmorpholine N-oxide (NMO), can enhance the catalytic cycle by promoting oxidation of the Ru center. Ru(III) complexes may also be compatible with aqueous or mixed solvent systems in some oxidation reactions, allowing for mild and environmentally friendly conditions in green chemistry applications.
- Substrate Compatibility: Ru(III) complexes are versatile and can oxidize extensive range of substrates, including alcohols, alkenes, and sulfides. Their flexibility in oxidation states allows for efficient oxidation of functional groups, making them suitable for selective transformations in both small-molecule synthesis and complex organic molecules. They are particularly effective with substrates requiring precise control over oxidative transformations, such as in production of fine chemicals and pharmaceuticals.

Palladium (II)

- Temperature: Pd(II) complexes are typically used at lower to moderate temperatures (25–80°C), particularly in carbon-carbon coupling reactions, which require milder conditions to prevent catalyst degradation and side reactions. Lower temperatures help maintain Pd(II) in its stable oxidation state, supporting oxidative addition and reductive elimination without promoting unwanted Pd(0) aggregation.

- Solvent: Palladium (II) complexes are often employed in polar, aprotic solvents like tetrahydrofuran (THF), toluene, and dimethylformamide (DMF). In some cases, aqueous-organic solvent mixtures are used, especially in Suzuki-Miyaura couplings, as they improve the solubility of reagents and products. The solvent choice is critical in Pd-catalyzed coupling reactions since it affects the solubility and reactivity of both the metal complex and organic substrates. A base, such as K_2CO_3 or NaOAc, is frequently added to facilitate the reaction and stabilize Pd intermediates.
- Substrate Compatibility: Pd(II) complexes are perfect for cross-coupling reactions (such as Suzuki, Heck, and Sonogashira reactions) because they work very well with substrates that include carbon-halide bonds. By facilitating creation of C-C as well as C-N bonds, these complexes enable aryl halides to be coupled with other partners or organometallic reagents. Thus, palladium complexes are frequently used in organic synthesis to create intricate molecular structures, particularly in pharmaceutical and materials chemistry.

Ru(III) complexes thrive in conditions that support redox flexibility and high-temperature reactions, ideal for oxidation processes. Conversely, Pd(II) complexes operate under milder conditions favoring stability, making them suitable for precise cross-coupling reactions in organic synthesis(70).

5. CONCLUSION

The Ruthenium(III) N_2O_2 Schiff base complexes demonstrate higher catalytic efficiency than Palladium(II) counterparts, particularly in oxidation reactions. This efficiency stems from Ruthenium(III)'s adaptable redox properties and versatile coordination geometry, which allow for rapid electron transfer and support diverse catalytic cycles. Unlike Palladium(II) complexes, which are well-suited for carbon-carbon coupling due to their stability in a single oxidation state, Ruthenium(III) complexes thrive in redox-driven environments where shifts between oxidation states enhance catalytic turnover and reaction selectivity. This review underscores the distinctive qualities of Ruthenium(III) complexes, emphasizing their potential in applications requiring efficient oxidation, such as fine chemical synthesis and environmental catalysis. Furthermore, the comparative analysis provided here offers valuable insights into optimizing Schiff base ligands for even greater efficiency. By tailoring ligand structures to further stabilize reactive intermediates and facilitate specific reaction pathways, researchers could unlock new catalytic capabilities for both Ru(III) and Pd(II) complexes. This understanding opens avenues for future studies to refine these catalysts, exploring sustainable, high-performance catalytic systems that leverage the unique strengths of each metal-ligand configuration. Such research will drive progress in green chemistry and industrial catalysis, contributing to more effective and environmentally responsible chemical processes.

5.1. Future Directions

Future directions for research on Schiff base complexes involving Ruthenium(III) and Palladium(II) should focus on three key areas: ligand modification and design, asymmetric oxidation reactions, and sustainable catalytic systems. First, by exploring ligand modifications, scientists can refine the selectivity and efficiency of these metal complexes, tailoring them to specific substrates and reactions. This involves designing ligands that enhance catalytic performance through optimized coordination and redox properties, expanding the potential applications in oxidation and reduction processes. Second, advancing asymmetric oxidation reactions will allow for selective transformations in complex organic synthesis, particularly for chiral compounds in pharmaceuticals. Developing these reactions with Schiff base complexes holds promise for high selectivity and efficiency. Lastly, creating sustainable and efficient catalytic systems aligns with current environmental priorities by minimizing waste and energy consumption. This can be achieved by exploring green solvents, reusable catalysts, and eco-friendly reaction conditions, promoting the long-term applicability of these metal complexes in industrial settings. These directions hold the potential to significantly advance the field of catalysis using Schiff base metal complexes.

Reference:

1. Meena, R., Meena, P., Kumari, A., Sharma, N., & Fahmi, N. (2023). Schiff bases and their metal complexes: Synthesis, structural characteristics and applications. In *Schiff Base in Organic, Inorganic and Physical Chemistry*. IntechOpen.
2. Q. Memon, S., Memon, N., Mallah, A., Soomro, R., & Y. Khuhawar, M. (2014). Schiff bases as chelating reagents for metal ions analysis. *Current Analytical Chemistry*, *10*(3), 393-417.

3. Nworie, F., Nwabue, F., Elom, N., & Eluu, S. (2016). Schiff bases and schiff base metal complexes: from syntheses to applications. *Journal of Basic and Applied Research in Biomedicine*, *2*(3), 295-305.
4. Shariff, S. N., Saravu, S., & Ramakrishna, D. (2022). Schiff Base complexes for catalytic application. In *Schiff Base in Organic, Inorganic and Physical Chemistry*. IntechOpen.
5. Segura, J. L., Mancheño, M. J., & Zamora, F. (2016). Covalent organic frameworks based on Schiff-base chemistry: synthesis, properties and potential applications. *Chemical Society Reviews*, *45*(20), 5635-5671.
6. Raja, K. K., Gandhi, N. I., Lekha, L., Easwaramoorthy, D., & Rajagopal, G. (2014). Synthesis, spectral, electrochemical and catalytic properties of Ru (III) Schiff base complexes containing N, O donors. *Journal of Molecular Structure*, *1060*, 49-57.
7. Thangadurai, T. D., & Ihm, S. K. (2004). Novel bidentate ruthenium (III) Schiff base complexes: synthetic, spectral, electrochemical, catalytic and antimicrobial studies. *Transition metal chemistry*, *29*(2), 189-195.
8. Kargar, H., Fallah-Mehrjardi, M., Behjatmanesh-Ardakani, R., Bahadori, M., Moghadam, M., Ashfaq, M., ... & Tahir, M. N. (2022). Spectroscopic investigation, molecular structure, catalytic activity with computational studies of a novel Pd (II) complex incorporating unsymmetrical tetradentate Schiff base ligand. *Inorganic Chemistry Communications*, *142*, 109697.
9. Pratihar, J. L., Mandal, P., Lai, C. K., & Chattopadhyay, S. (2019). Tetradentate amido azo Schiff base Cu (II), Ni (II) and Pd (II) complexes: Synthesis, characterization, spectral properties, and applications to catalysis in C–C coupling and oxidation reaction. *Polyhedron*, *161*, 317-324.
10. Venkatachalam, G., Raja, N., Pandiarajan, D., & Ramesh, R. (2008). Binuclear ruthenium (III) Schiff base complexes bearing N4O4 donors and their catalytic oxidation of alcohols. *Spectrochimica Acta Part A: Molecular and Biomolecular Spectroscopy*, *71*(3), 884-891.
11. Ramesh, R. (2004). Spectral and catalytic studies of ruthenium (III) Schiff base complexes. *Inorganic Chemistry Communications*, *7*(2), 274-276.
12. Ramesh, R., & Maheswaran, S. (2003). Synthesis, spectra, dioxygen affinity and antifungal activity of Ru (III) Schiff base complexes. *Journal of inorganic biochemistry*, *96*(4), 457-462.
13. Venkatachalam, G., Raja, N., Pandiarajan, D., & Ramesh, R. (2008). Binuclear ruthenium (III) Schiff base complexes bearing N4O4 donors and their catalytic oxidation of alcohols. *Spectrochimica Acta Part A: Molecular and Biomolecular Spectroscopy*, *71*(3), 884-891.
14. Venkatachalam, G., Raja, N., Pandiarajan, D., & Ramesh, R. (2008). Binuclear ruthenium (III) Schiff base complexes bearing N4O4 donors and their catalytic oxidation of alcohols. *Spectrochimica Acta Part A: Molecular and Biomolecular Spectroscopy*, *71*(3), 884-891.
15. Venkatachalam, G., Raja, N., Pandiarajan, D., & Ramesh, R. (2008). Binuclear ruthenium (III) Schiff base complexes bearing N4O4 donors and their catalytic oxidation of alcohols. *Spectrochimica Acta Part A: Molecular and Biomolecular Spectroscopy*, *71*(3), 884-891.
16. Tang, L. H., Wu, F., Lin, H., Jia, A. Q., & Zhang, Q. F. (2018). Synthesis, structure and catalytic alcohol oxidation by ruthenium (III) supported by Schiff base and triphenylphosphine ligands. *Inorganica Chimica Acta*, *477*, 212-218.
17. Choi, S., Yang, J. D., Ji, M., Choi, H., Kee, M., Ahn, K. H., ... & Koo, S. (2001). Selective oxidation of allylic sulfides by hydrogen peroxide with the trirutile-type solid oxide catalyst LiNbMoO6. *The Journal of Organic Chemistry*, *66*(24), 8192-8198.
18. Murahashi, S. I., & Komiya, N. (2004). Ruthenium-catalyzed Oxidation of Alkenes, Alcohols, Amines, Amides, b-Lactams, Phenols, and Hydrocarbons. *Modern Oxidation Methods*.
19. Bergstad, K., & Bäckvall, J. E. (1998). Mild and efficient flavin-catalyzed H2O2 oxidation of tertiary amines to amine N-oxides. *The Journal of Organic Chemistry*, *63*(19), 6650-6655.
20. Boring, E., Geletii, Y. V., & Hill, C. L. (2001). A homogeneous catalyst for selective O2 oxidation at ambient temperature. Diversity-based discovery and mechanistic investigation of thioether oxidation by the Au (III) Cl2NO3 (thioether)/O2 system. *Journal of the American Chemical Society*, *123*(8), 1625-1635.
21. Murahashi, S. I., & Komiya, N. (2004). Ruthenium-catalyzed Oxidation of Alkenes, Alcohols, Amines, Amides, b-Lactams, Phenols, and Hydrocarbons. *Modern Oxidation Methods*.
22. Li, T. T., Li, F. M., Zhao, W. L., Tian, Y. H., Chen, Y., Cai, R., & Fu, W. F. (2015). Highly Efficient and Selective Photocatalytic Oxidation of Sulfide by a Chromophore–Catalyst Dyad of Ruthenium-Based Complexes. *Inorganic Chemistry*, *54*(1), 183-191.

23. Li, T. T., Li, F. M., Zhao, W. L., Tian, Y. H., Chen, Y., Cai, R., & Fu, W. F. (2015). Highly Efficient and Selective Photocatalytic Oxidation of Sulfide by a Chromophore–Catalyst Dyad of Ruthenium-Based Complexes. *Inorganic Chemistry*, *54*(1), 183-191.
24. Li, T. T., Li, F. M., Zhao, W. L., Tian, Y. H., Chen, Y., Cai, R., & Fu, W. F. (2015). Highly Efficient and Selective Photocatalytic Oxidation of Sulfide by a Chromophore–Catalyst Dyad of Ruthenium-Based Complexes. *Inorganic Chemistry*, *54*(1), 183-191.
25. Andreu, M. G., Zapf, A., & Beller, M. (2000). Molecularly defined palladium (0) monophosphine complexes as catalysts for efficient cross-coupling of aryl chlorides and phenylboronic acid1. *Chemical Communications*, (24), 2475-2476.
26. Karvembu, R., Jayabalakrishnan, C., Dharmaraj, N., Renukadevi, S. V., & Natarajan, K. (2002). Binuclear ruthenium (III) complexes: synthesis, characterisation, catalytic activity in aryl–aryl couplings and biological activity. *Transition metal chemistry*, *27*, 631-638.
27. Karvembu, R., Jayabalakrishnan, C., Dharmaraj, N., Renukadevi, S. V., & Natarajan, K. (2002). Binuclear ruthenium (III) complexes: synthesis, characterisation, catalytic activity in aryl–aryl couplings and biological activity. *Transition metal chemistry*, *27*, 631-638.
28. Jayabalakrishnan, C., Karvembu, R., & Natarajan, K. (2003). Ruthenium (III) Schiff Base Complexes: Catalytic Activity in Aryl–Aryl Coupling Reaction and Antimicrobial Activity. *Synthesis and reactivity in inorganic and metal-organic chemistry*, *33*(9), 1535-1553.
29. Jayabalakrishnan, C., Karvembu, R., & Natarajan, K. (2003). Ruthenium (III) Schiff Base Complexes: Catalytic Activity in Aryl–Aryl Coupling Reaction and Antimicrobial Activity. *Synthesis and reactivity in inorganic and metal-organic chemistry*, *33*(9), 1535-1553.
30. Jayabalakrishnan, C., Karvembu, R., & Natarajan, K. (2003). Ruthenium (III) Schiff Base Complexes: Catalytic Activity in Aryl–Aryl Coupling Reaction and Antimicrobial Activity. *Synthesis and reactivity in inorganic and metal-organic chemistry*, *33*(9), 1535-1553.
31. Quan, M., Sanchez, D.,Wasylkiw, M. F., & Smith, D. K. (2007). Voltammetry of quinones in unbuffered aqueous solution: reassessing the roles of proton transfer and hydrogen bonding in the aqueous electrochemistry of quinones. *Journal of the American Chemical Society*, *129*(42), 12847-12856.
32. Quan, M., Sanchez, D.,Wasylkiw, M. F., & Smith, D. K. (2007). Voltammetry of quinones in unbuffered aqueous solution: reassessing the roles of proton transfer and hydrogen bonding in the aqueous electrochemistry of quinones. *Journal of the American Chemical Society*, *129*(42), 12847-12856.
33. He, Z., Colbran, S. B., & Craig, D. C. (2003). Could redox-switched binding of a redox-active ligand to a copper (ii) centre drive a conformational proton pump gate? A synthetic model study. *Chemistry–A European Journal*, *9*(1), 116-129.
34. Lonnon, D. G., Lee, S. T., & Colbran, S. B. (2007). Valence Tautomerism and Coordinative Lability in Copper (II)− Imidazolyl− Semiquinonate Anion Radical Models for the CuB Center in Cytochrome c Oxidases. *Journal of the American Chemical Society*, *129*(18), 5800-5801.
35. He, Z., Colbran, S. B., & Craig, D. C. (2003). Could redox-switched binding of a redox-active ligand to a copper (ii) centre drive a conformational proton pump gate? A synthetic model study. *Chemistry–A European Journal*, *9*(1), 116-129.
36. Quan, M., Sanchez, D., Wasylkiw, M. F., & Smith, D. K. (2007). Voltammetry of quinones in unbuffered aqueous solution: reassessing the roles of proton transfer and hydrogen bonding in the aqueous electrochemistry of quinones. *Journal of the American Chemical Society*, *129*(42), 12847-12856.
37. Colbran, S. B., Lee, S. T., Lonnon, D. G., Maharaj, F. J., McDonagh, A. M., Walker, K. A., & Young, R. D. (2006). Covalently linked ferrocenyl quinones: Proton-dependent redox behavior and charge redistribution. *Organometallics*, *25*(9), 2216-2224.
38. Berben, L. A., Craig, D. C., Gimbert-Suriñach, C., Robinson, A., Sugiyarto, K. H., & Colbran, S. B. (2011). Palladium (II) complexes of imidazolin-2-ylidene N-heterocyclic carbene ligands with redox-active dimethoxyphenyl or (hydro) quinonyl substituents. *Inorganica Chimica Acta*, *370*(1), 374-381.
39. Berben, L. A., Craig, D. C., Gimbert-Suriñach, C., Robinson, A., Sugiyarto, K. H., & Colbran, S. B. (2011). Palladium (II) complexes of imidazolin-2-ylidene N-heterocyclic carbene ligands with re-

dox-active dimethoxyphenyl or (hydro) quinonyl substituents. *Inorganica Chimica Acta*, *370*(1), 374-381.

40. Berben, L. A., Craig, D. C., Gimbert-Suriñach, C., Robinson, A., Sugiyarto, K. H., & Colbran, S. B. (2011). Palladium (II) complexes of imidazolin-2-ylidene N-heterocyclic carbene ligands with redox-active dimethoxyphenyl or (hydro) quinonyl substituents. *Inorganica Chimica Acta*, *370*(1), 374-381.
41. Mane, P. A., Dey, S., & Vivekananda, K. V. (2017). Macrocyclic Pd (II) dithiolate complexes as catalysts in Heck reactions. *Tetrahedron Letters*, *58*(1), 25-29.
42. Vivekananda, K. V., Dey, S., Maity, D. K., Bhuvanesh, N., & Jain, V. K. (2015). Supramolecular Macrocyclic Pd (II) and Pt (II) Squares and Rectangles with Aryldithiolate Ligands and their Excellent Catalytic Activity in Suzuki C–C Coupling Reaction. *Inorganic Chemistry*, *54*(21), 10153-10162.
43. Mane, P. A., Dey, S., Pathak, A. K., Kumar, M., & Bhuvanesh, N. (2019). Xantphos-Capped Pd (II) and Pt (II) Macrocycles of Aryldithiolates: Structural Variation and Catalysis in C–C Coupling Reaction. *Inorganic Chemistry*, *58*(5), 2965-2978.
44. Gaikwad, V. V., Mane, P. A., Dey, S., & Bhanage, B. M. (2019). Dppf-Ligated Palladium Complex as an Efficient Catalyst for the Synthesis of Biaryl Ketones Using Co2 (CO) 8 as a C1 Source with High TON and TOF. *ChemistrySelect*, *4*(28), 8269-8276.
45. Gaikwad, V. V., Mane, P. A., Dey, S., & Bhanage, B. M. (2019). Dppf-Ligated Palladium Complex as an Efficient Catalyst for the Synthesis of Biaryl Ketones Using Co2 (CO) 8 as a C1 Source with High TON and TOF. *ChemistrySelect*, *4*(28), 8269-8276.
46. Gaikwad, V. V., Mane, P. A., Dey, S., & Bhanage, B. M. (2019). Dppf-Ligated Palladium Complex as an Efficient Catalyst for the Synthesis of Biaryl Ketones Using Co2 (CO) 8 as a C1 Source with High TON and TOF. *ChemistrySelect*, *4*(28), 8269-8276.
47. Kočovský, P., & Bäckvall, J. E. (2015). The syn/anti-dichotomy in the palladium-catalyzed addition of nucleophiles to alkenes. *Chemistry–A European Journal*, *21*(1), 36-56.
48. Keith, J. A., & Henry, P. M. (2009). The mechanism of the Wacker reaction: a tale of two hydroxypalladations. *Angewandte Chemie International Edition*, *48*(48), 9038-9049.
49. Mann, S. E., Benhamou, L., & Sheppard, T. D. (2015). Palladium (II)-catalysed oxidation of alkenes. *Synthesis*, *47*(20), 3079-3117.
50. Mann, S. E., Benhamou, L., & Sheppard, T. D. (2015). Palladium (II)-catalysed oxidation of alkenes. *Synthesis*, *47*(20), 3079-3117.
51. Khabibulin, V. R., Kulik, A. V., Oshanina, I. V., Bruk, L. G., Temkin, O. N., Nosova, V. M., ... & Antipin, M. Y. (2007). Mechanism of the oxidative carbonylation of terminal alkynes at the≡ CH bond in solutions of palladium complexes. *Kinetics and Catalysis*, *48*, 228-244.
52. Khabibulin, V. R., Kulik, A. V., Oshanina, I. V., Bruk, L. G., Temkin, O. N., Nosova, V. M., ... & Antipin, M. Y. (2007). Mechanism of the oxidative carbonylation of terminal alkynes at the≡ CH bond in solutions of palladium complexes. *Kinetics and Catalysis*, *48*, 228-244.
53. Khabibulin, V. R., Kulik, A. V., Oshanina, I. V., Bruk, L. G., Temkin, O. N., Nosova, V. M., ... & Antipin, M. Y. (2007). Mechanism of the oxidative carbonylation of terminal alkynes at the≡ CH bond in solutions of palladium complexes. *Kinetics and Catalysis*, *48*, 228-244.
54. Pattanayak, P., Pratihar, J. L., Patra, D., Lin, C. H., Paul, S., & Chakraborty, K. (2013). Synthesis, characterization, structure, redox property, antibacterial and catalytic activity of tridentate Schiff base cobalt (III), nickel (II) and palladium (II) complexes. *Polyhedron*, *51*, 275-282.
55. Pattanayak, P., Pratihar, J. L., Patra, D., Lin, C. H., Paul, S., & Chakraborty, K. (2013). Synthesis, characterization, structure, redox property, antibacterial and catalytic activity of tridentate Schiff base cobalt (III), nickel (II) and palladium (II) complexes. *Polyhedron*, *51*, 275-282.

56. Pattanayak, P., Pratihar, J. L., Patra, D., Lin, C. H., Paul, S., & Chakraborty, K. (2013). Synthesis, characterization, structure, redox property, antibacterial and catalytic activity of tridentate Schiff base cobalt (III), nickel (II) and palladium (II) complexes. *Polyhedron*, *51*, 275-282.
57. Pattanayak, P., Pratihar, J. L., Patra, D., Lin, C. H., Paul, S., & Chakraborty, K. (2013). Synthesis, characterization, structure, redox property, antibacterial and catalytic activity of tridentate Schiff base cobalt (III), nickel (II) and palladium (II) complexes. *Polyhedron*, *51*, 275-282.

58. Ejidike, I. P., & Ajibade, P. A. (2016). Ruthenium (III) complexes of heterocyclic tridentate (ONN) Schiff base: Synthesis, characterization and its biological properties as an antiradical and antiproliferative agent. *International Journal of Molecular Sciences*, *17*(1), 60.
59. Ejidike, I. P., & Ajibade, P. A. (2016). Ruthenium (III) complexes of heterocyclic tridentate (ONN) Schiff base: Synthesis, characterization and its biological properties as an antiradical and antiproliferative agent. *International Journal of Molecular Sciences*, *17*(1), 60.
60. Ejidike, I. P., & Ajibade, P. A. (2016). Ruthenium (III) complexes of heterocyclic tridentate (ONN) Schiff base: Synthesis, characterization and its biological properties as an antiradical and antiproliferative agent. *International Journal of Molecular Sciences*, *17*(1), 60.
61. Souza, M. L., Castellano, E. E., Telser, J., & Franco, D. W. (2015). Secondary coordination sphere effects in ruthenium (III) tetraammine complexes: role of the coordinated water molecule. *Inorganic Chemistry*, *54*(4), 2067-2080.
62. Souza, M. L., Castellano, E. E., Telser, J., & Franco, D. W. (2015). Secondary coordination sphere effects in ruthenium (III) tetraammine complexes: role of the coordinated water molecule. *Inorganic Chemistry*, *54*(4), 2067-2080.
63. Kargar, H., Torabi, V., Akbari, A., Behjatmanesh-Ardakani, R., & Tahir, M. N. (2019). Synthesis, characterization, crystal structure and DFT studies of a palladium (II) complex with an asymmetric Schiff base ligand. *Journal of Molecular Structure*, *1179*, 732-738.
64. Kargar, H., Torabi, V., Akbari, A., Behjatmanesh-Ardakani, R., & Tahir, M. N. (2019). Synthesis, characterization, crystal structure and DFT studies of a palladium (II) complex with an asymmetric Schiff base ligand. *Journal of Molecular Structure*, *1179*, 732-738.
65. Kargar, H., Torabi, V., Akbari, A., Behjatmanesh-Ardakani, R., & Tahir, M. N. (2019). Synthesis, characterization, crystal structure and DFT studies of a palladium (II) complex with an asymmetric Schiff base ligand. *Journal of Molecular Structure*, *1179*, 732-738.
66. Kargar, H., Torabi, V., Akbari, A., Behjatmanesh-Ardakani, R., & Tahir, M. N. (2019). Synthesis, characterization, crystal structure and DFT studies of a palladium (II) complex with an asymmetric Schiff base ligand. *Journal of Molecular Structure*, *1179*, 732-738.
67. Kargar, H., Torabi, V., Akbari, A., Behjatmanesh-Ardakani, R., & Tahir, M. N. (2019). Synthesis, characterization, crystal structure and DFT studies of a palladium (II) complex with an asymmetric Schiff base ligand. *Journal of Molecular Structure*, *1179*, 732-738.
68. Kargar, H., Torabi, V., Akbari, A., Behjatmanesh-Ardakani, R., & Tahir, M. N. (2019). Synthesis, characterization, crystal structure and DFT studies of a palladium (II) complex with an asymmetric Schiff base ligand. *Journal of Molecular Structure*, *1179*, 732-738.
69. Said, M. A., Al-unizi, A., Al-Mamary, M., Alzahrani, S., & Lentz, D. (2020). Easy coordinate geometry indexes, $\tau 4$ and $\tau 5$ and HSA study for unsymmetrical Pd (II), Fe (II), Zn (II), Mn (II), Cu (II) and VO (IV) complexes of a tetradentate ligand: Synthesis, characterization, properties, and antioxidant activities. *Inorganica Chimica Acta*, *505*, 119434.
70. Subarkhan, M. M., & Ramesh, R. (2015). Binuclear ruthenium (III) bis (thiosemicarbazone) complexes: Synthesis, spectral, electrochemical studies and catalytic oxidation of alcohol. *Spectrochimica Acta Part A: Molecular and Biomolecular Spectroscopy*, *138*, 264-270.